Accepted Manuscript

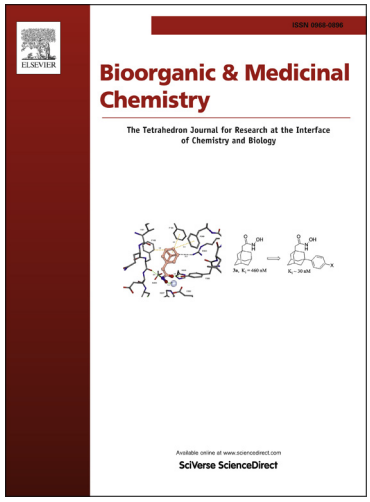

Synthesis and antiproliferative activity of conformationally restricted 1,2,3-triazole analogues of combretastatins in the sea urchin embryo model and against human cancer cell lines

Dmitry V. Demchuk, Alexander V. Samet, Natalia B. Chernysheva, Vladimir I. Ushkarov, Galina A. Stashina, Leonid D. Konyushkin, Mikhail M. Raihstat, Sergei I. Firgang, Alex A. Philchenkov, Michael P. Zavelevich, Ludmila M. Kuiava, Vasyl F. Chekhun, Dmitry Yu. Blokhin, Alex S. Kiselyov, Marina N. Semenova, Victor V. Semenov

PII: S0968-0896(13)01009-2
DOI: http://dx.doi.org/10.1016/j.bmc.2013.12.015
Reference: BMC 11277

To appear in: *Bioorganic & Medicinal Chemistry*

Received Date: 13 October 2013
Revised Date: 1 December 2013
Accepted Date: 6 December 2013

Please cite this article as: Demchuk, D.V., Samet, A.V., Chernysheva, N.B., Ushkarov, V.I., Stashina, G.A., Konyushkin, L.D., Raihstat, M.M., Firgang, S.I., Philchenkov, A.A., Zavelevich, M.P., Kuiava, L.M., Chekhun, V.F., Blokhin, D.Y., Kiselyov, A.S., Semenova, M.N., Semenov, V.V., Synthesis and antiproliferative activity of conformationally restricted 1,2,3-triazole analogues of combretastatins in the sea urchin embryo model and against human cancer cell lines, *Bioorganic & Medicinal Chemistry* (2013), doi: http://dx.doi.org/10.1016/j.bmc.2013.12.015

Synthesis and antiproliferative activity of conformationally restricted 1,2,3-triazole analogues of combretastatins in the sea urchin embryo model and against human cancer cell lines

Dmitry V. Demchuk [a], Alexander V. Samet [a], Natalia B. Chernysheva [a], Vladimir I. Ushkarov [a], Galina A. Stashina [a], Leonid D. Konyushkin [a], Mikhail M. Raihstat [a,b], Sergei I. Firgang [a], Alex A. Philchenkov [c], Michael P. Zavelevich [c], Ludmila M. Kuiava [c], Vasyl F. Chekhun [c], Dmitry Yu. Blokhin [d], Alex S. Kiselyov [e], Marina N. Semenova [b,f], Victor V. Semenov [a,b,*]

[a] *N. D. Zelinsky Institute of Organic Chemistry RAS, 47 Leninsky Prospect, 119991 Moscow, Russian Federation*

[b] *Chemical Block Ltd., 3 Kyriacou Matsi, 3723 Limassol, Cyprus*

[c] *R. E. Kavetsky Institute of Experimental Oncology, Pathology and Radiobiology, National Academy of Sciences of Ukraine, 45 Vasyl'kivska Street, 03022 Kyiv, Ukraine*

[d] *N. N. Blokhin Cancer Research Center, 24 Kashirskoe Shosse, 115478 Moscow, Russian Federation*

[e] *ChemDiv, 6605 Nancy Ridge Drive, San Diego, CA 92121, USA*

[f] *N. K. Kol'tsov Institute of Developmental Biology RAS, 26 Vavilov Street, 119334 Moscow, Russian Federation*

Dmitry V. Demchuk demchuk@ioc.ac.ru
Alexander V. Samet sametav@ioc.ac.ru
Natalia B. Chernysheva info@chemblock.com
Vladimir I. Ushkarov ushkarov@inbox.ru
Galina A. Stashina galina_stashina@chemical-block.com
Leonid D. Konyushkin LeonidK@chemical-block.com
Mikhail M. Raihstat mr@chemical-block.com
Sergei I. Firgang cbi@chemical-block.com
Alex A. Philchenkov a_philch@onconet.kiev.ua
Michael P. Zavelevich butenko@onconet.kiev.ua
Ludmila M. Kuiava kuyavalm@ukr.net
Vasiliy F. Chekhun chekhun@onconet.kiev.ua
Dmitry Yu. Blokhin blokhin@yandex.ru
Alex S. Kiselyov akiselyov@chemdiv.com
Marina N. Semenova ms@chemical-block.com
Victor V. Semenov vs@zelinsky.ru

[*] To whom correspondence should be addressed. Tel: +7 (916) 620-9584. Fax: +7 (499) 137-2966. E-mail: vs@zelinsky.ru

Abbreviations:

Bcl-2, B-cell lymphoma 2; CA2, combretastatin A-2; CA4, combretastatin A-4; CA4P, CA4 disodium phosphate; MoAb, monoclonal antibody; PARP-1, poly(ADP-ribose) polymerase-1; PI, propidium iodide; SAR, structure-activity relationship; XIAP, X-linked inhibitor of apoptosis

Key words:

1,2,3-Triazole

Apoptosis

Caspases

Plant polyalkoxybenzenes

Microtubule destabilizing agents

Sea urchin embryo

Abstract

A series of 1,5-diaryl- and 4,5-diaryl-1,2,3-triazole derivatives of combretastatin A4 were synthesized and evaluated as antimitotic microtubule destabilizing agents using the sea urchin embryo model. Structure-activity relationship studies identified compounds substituted with 3,4,5-trimethoxyphenyl and 3,4-methylenedioxy-5-methoxyphenyl ring A and 4-methoxyphenyl ring B as potent antiproliferative agents with high cytotoxicity against a panel of human cancer cell lines including multi-drug resistant cells. 4,5-Diaryl-1,2,3-triazoles (C–C geometry) were found to be considerably more active than the respective 1,5-diaryl-1,2,3-triazoles (N–C geometry). Compound **10ad'** induced G_2/M cell cycle arrest and apoptosis in human T-leukemia Jurkat cells *via* caspase 2/3/9 activation and downregulation of the antiapoptotic protein XIAP. A mitotic catastrophe has been evaluated as another possible cell death mode.

1. Introduction

Natural antimitotic stilbenes represented by combretastatins A-1, A-2 and A-4 (Fig. 1; CA1, CA2, and CA4) are constituents of the bark of the African willow tree *Combretum caffrum* Kuntze (Combretaceae).[1–3] These molecules are strong inhibitors of tubulin polymerization interacting with the colchicine binding site of tubulin.[4,5] CA4 and its derivatives are potently cytotoxic against a wide variety of human solid tumor and hematological malignancies both *in vitro* and *in vivo*. Water-soluble phosphorylated prodrugs CA4 disodium phosphate (CA4P, Zybrestat) and combretastatin A-1 disodium phosphate (Oxi4503) (Fig. 1) are currently in clinical trials as antitumor vascular disrupting agents.[6–9] However, these drugs affect cardiovascular system, cause acute pain, and display other serious side effects limiting their therapeutic utility.[10–12] A significant efforts were dedicated to the design and development of novel conformationally restricted combretastatin analogues with reduced general toxicity and improved on-target efficacy profiles.[13,14]

Insert Figure 1

Numerous reports suggest that only *cis*-conformation of combretastatins and its analogues is relevant to their cytotoxic, antimitotic, and antitubulin activity.[13–15] Unfortunately, isomerization to the inactive *trans*-configuration happens spontaneously upon exposure to heat, light, and protic media. Importantly, *cis-trans* biotransformation has also been reported as one of metabolic pathways of CA4 in liver microsomes.[16] A relatively simple chemical structure of combretastatins provides opportunity for the development of a large number of biologically active stilbenes by 'locking' the olefinic bond into the respective non-isomerizable scaffold.[13,14] For example, various 5-membered *N*-containing heterocyclic templates including 4,5-diaryloxazoles,[17] isoxasoles,[18,19] diarylthiazoles,[20] thiazol-2(3H)-ones,[21] imidazol-2-ones,[22] pyrazolones,[23] pyrazoles,[24,25] tetrazoles,[26] 1,2,4-[27,28], and 1,2,3-triazoles[29–34] were successful isosteres of the *cis*-olefin. The resulting compounds retained potency of the parent CA4 and exhibited favorable stability *ex vivo* and *in vivo*.

In addition to the *cis*-olefine linker, both the 3,4,5-trimethoxy substituted ring A and *p*-methoxy group in the ring B are essential for the antimitotic antitubulin effects of combretastatin series.[13,14] The position of 3,4,5-trimethoxyphenyl (A) and *p*-methoxyphenyl (B) rings relative to the heterocyclic isostere was shown to be important for biological activity.[13] *ortho*-Substituted diaryl azoles consistently displayed markedly higher antiproliferative activity than their *meta*-analogues.[31,33,35] Moreover, nature of the bond (N *vs* C linking) between these aryl substituents and N-heterocycle dramatically affected the activity of regioisomers, as shown for 1,2,3-triazole,[30,31,33] 1,2,4-triazole,[28] and tetrazole[36] series. Specifically, the attachment of the trimethoxy substituted ring A to nitrogen yielded considerably more potent compounds.

When analyzing the literature on heterocyclic analogues of combretastatins, we noticed that the systematic structure-activity relationship (SAR) linking the effect of a substituent in the heterocyclic bridge (amino-, alkyl-, and other groups) to the cytotoxic properties of the resultant molecule are somewhat scarce and controversial. For instance, it was found that the introduction of CH_3 or NH_2 groups into triazole bridge of 3,4-diaryl-1,2,4-triazoles resulted in the loss of activity.[37] However, 4,5-diaryl-3-aminopyrazoles[24,25] and 3,4-diaryl-5-aminoisoxazoles[21] were reported to display significant cytotoxicity, cell cycle arrest in G2/M phase, and inhibition of tubulin polymerization. Similarly, both 3,4-diaryl-5-amino- and 4,5-diaryl-3-aminoisoxazoles exhibited high antimitotic microtubule destabilizing activity, whereas *N*-acetylation of the NH_2 group in these series yielded ambiguous results.[21,38]

Considering the above literature evidence, we aimed to study the impact of substitution in the i) heterocycle isostere; ii) aromatic rings A and B, and iii) relative position of the A and B rings on the biological activity of *cis*-restricted combretastatin analogues. *Ortho*-diaryl-substituted 1,2,3-triazoles (Fig. 1) featuring aromatic rings connected to either N-C (1,5-geometry) or C-C (4,5-geometry) atoms of the heterocycles were selected for several reasons. First, 1,5-diaryl-1,2,3-triazoles were described to be potent cytotoxic agents affecting tubulin polymerization.[30–34,39] Second, a single position in 1,5-

diaryl-1,2,3-triazoles is available for substitution minimizing the number of possible regioisomers. Third, biological activity of 4,5-diaryl-1,2,3-triazoles was not reported in great detail.[29,39] Particularly, CA4 and its derivatives were reported to kill malignant cells by inducing different modes of cell death including apoptosis,[35,36,40] necrosis,[41] autophagy,[42] and mitotic catastrophe.[43] However, the question remains, is there any relationship between cell type, cell death mechanism, and chemical structure of antimitotic stilbenes.

In the present study we decided to: (i) conduct structure-activity relationship (SAR) studies for 1,5-diaryl-1,2,3-triazole series in order to identify the optimized substitution pattern within this structural class; (ii) estimate the antiproliferative and microtubule destabilizing activity using phenotypic sea urchin embryo assay[44]; (iii) compare antimitotic activity of 1,5- and 4,5-diaryl-1,2,3-triazoles, and (iv) assess cytotoxicity and apoptosis inducing properties of these series in cultured human cancer cells. Triggering of apoptosis was studied using Jurkat human leukemia T-cells and its multi-drug resistant subclone Jurkat A4.

The resistance of tumors to chemotherapeutics, including microtubule targeting drugs, is a substantial problem in oncology. In 2001, Jurkat/A4 subclone was obtained by exposure of Jurkat human leukemia T-cells to agonistic monoclonal antibodies (MoAb) against the death receptor Fas (CD95/APO-1) and selection of survived cells lacking functional Fas on their surface.[45] Jurkat/A4 cells displayed resistance toward several anticancer drugs such as etoposide, doxorubicin, and cycloplatam, as well as to various apoptotic stimuli, including UV-irradiation, lethal doses of X-rays, oxidative stress (H_2O_2 and menadione), protein kinase inhibitor staurosporin, and tumor necrosis factor-related apoptosis-inducing ligand TRAIL (despite the presence of the TRAIL receptor DR5). Therefore, Jurkat/A4 cells represent a promising model to study molecular mechanisms of multi-drug resistance,

in particular, inability to execute apoptotic cell death, that may be useful in screening for compounds capable of killing resistant cells.

Previously it was shown that the sea urchin embryo model provides reliable and reproducible evaluation of solubility in salt-containing medium (seawater), cell permeability, antimitotic potential, and general toxicity/embryotoxicity of tested molecules together with their mode of action. The assay includes (i) fertilized egg test for antimitotic activity assessed by cleavage alteration/arrest and (ii) behavioral monitoring of a free-swimming hatched blastulae exposed to compounds. Specific changes of swimming pattern, namely, cessation of forward movement, settlement to the bottom of the culture vessel, and rapid spinning of an embryo around the animal–vegetal axis suggests a microtubule destabilizing activity caused by a molecule (video illustrations are available at http://www.chemblock.com). The reliability of data obtained by the sea urchin embryo assay has been verified by multiple conventional cell-based and tubulin polymerization assays.[46–48]

2. Results and discussion

2.1. Chemical synthesis

Polymethoxy substituted 1,5-diaryltriazoles **5**–**10** have been prepared *via* reported procedures from the respective aldehydes (Scheme 1). These were prepared as described earlier from the natural substrates isolated from the dill and parsley seed extracts.[49,50] Polymethoxy-4,5-diaryl-1,2,3-triazole analogues of combretastatin **14ad'**, **14bd'**, and **14cd'** have been prepared as described on Scheme 2.

Insert Schemes 1 and 2

1*H*-4,5-Diaryl-1,2,3-triazoles were prepared from corresponding benzaldehydes following a series of synthetic steps including 1) treatment of X with Ohira-Bestmann reagent; 2) Sonogashira coupling of the resulting acetylenes with 4-iodoanizole, and 3) [3+2]-cycloaddition of the acetylenes with benzylazide under high pressure and hydrogenation of the benzyl group. Our attempts to reduce reaction pressure or to use catalytic conditions to promote [3+2] cycloaddition step were unsuccessful. Specifically, the highest yields of the targeted 1*H*-4,5-diaryl-1,2,3-triazoles were secured when a solution of 1,2-diarylalkyne (2 mmol) and azide (2.60 mmol) in DMF (1 mL) was heated at 100 ºC and 15 kbar for 7 h (see Experimental section). Notably, the reaction did result in equal ratio (*ca.* 1:1)

regioisomers as evidenced by the NMR-analysis of crude reaction mixtures. In a representative experiment, the reaction mixture (isomers of 1-benzyl-4(5)-(4-methoxyphenyl)-5(4)-(3,4,5-trimethoxyphenyl)-1*H*-1,2,3-triazoles) was separated using column chromatography to furnish pure compound **13a'd**. Its structure was determined unequivocally using NOESY experiment. We observed an inter-space interaction of the *N*CH_2 with protons H-2''',6''' allowing to assign the structure of **13a'd**. The ^{1}H NMR signals of isomers in other mixtures were assigned in a similar way. Removal of the $PhCH_2$ fragment was accomplished by hydrogenation of the crude reaction mixtures at 20 bar. Since harsh reaction conditions required to access a series of 1*H*-4,5-diaryl-1,2,3-triazoles precluded us from completing the expanded structure-activity studies, we focused on synthesizing several representative compounds that were expected to parallel activities of the respective 1,5-diaryltriazoles. The main goal was to conduct a direct biological comparison of the most active analogues within these two classes of regioisomers.

2.2. Biological evaluation

2.2.1. Antimitotic activity in the phenotypic sea urchin embryo assay

The antiproliferative microtubule destabilizing effects of targeted *o*-diaryl-1,2,3-triazoles were studied in the phenotypic sea urchin embryo assay.[44] CA2 and CA4 served as reference compounds. The results are shown in Table 1.

Insert Table 1.

As evidenced from Table 1, 1,5-diaryl-1,2,3-triazoles **10ad'**, **10bd'**, and **5de'**, and 4,5-diaryl-1,2,3-triazoles **14ad'**, **14bd'**, and **14cd'** strongly affected sea urchin embryo cleavage and swimming behavior, causing embryo spinning. These phenotypic changes are directly related to antimitotic microtubule destabilizing activity of these compounds as shown by us earlier. The most potent molecules were substituted with trimethoxyphenyl- (**10ad'**) or 3,4-methylenedioxy-5-methoxyphenyl- (**10bd'**) (ring A) and *p*-methoxyphenyl groups (ring B). Tetramethoxy substitution in the ring A (**10cd'**) markedly reduced activity of the resultant molecules. Compounds **10da'** and **5fa'** could be considered

as antitubulin agents as well. Although they did not cause embryo spinning, the formation of tuberculate eggs typical of microtubule destabilizers was observed.[44,46,47]

Our sea urchin embryo data revealed that the substitution in the 1,2,3-triazole ring (**5ad'**–**9ad'**) was not tolerated as compared to the respective unsubstituted molecule **10ad'**. The introduction of 4-NH_2 group (**9ad'**) decreased activity, whereas addition of CN, $CONH_2$, $COOCH_3$, and COOH functionalities at C4 position afforded inactive compounds **5ad'**–**8ad'** (Табл. 1). It is worth noting that 1,5-diaryl-1,2,3-triazoles with trimethoxyphenyl ring A tethered to the *N* atom (**9ad'** and **10ad'**) were consistently more active than the respective regioisomers (trimethoxyphenyl substituent for the ring B, **9da'** and **10da'**). This fact is in a good agreement with the published evidence for the importance of trimethoxyphenyl ring A connection to a nitrogen atom in 1,5-diaryl-1,2,3-triazoles.[30,31,33]

4,5-Diaryl-1,2,3-triazoles **14ad'** and **14bd'** (C–C geometry) were found to be considerably more active than the respective 1,5-diaryl-1,2,3-triazoles **10ad'** and **10bd'** (N–C geometry). Similarly, compound **14cd'** displaying the tetra-substituted ring A exhibited only weak antiproliferative effect.

2.2.2. In vitro cancer cell growth inhibition

1,5-Diaryl-1,2,3-triazoles **5aa'**, **5dd'**, **5fa'**, **5fe'**, **6aa'**, **6ad'**, **7da'**, **8ad'**, **8da'**, **9da'**, and **10bd'**, and 4,5-diaryl-1,2,3-triazoles **14ad'**, **14bd'**, and **14cd'** have been further selected for cytotoxicity screen against 60 human tumor cell lines (Developmental Therapeutics Program at NCI). As anticipated, the data obtained by this cell-based assay correlated well with the sea urchin embryo observations (Tables 1 and 2). Namely, triazoles **5aa'**, **5dd'**, **5fe'**, **6aa'**, **6ad'**, **7da'**, **8ad'**, and **8da'**, inactive in the sea urchin embryos, did not inhibit cancer cell growth at concentrations up to 10 μM. Compounds **5fa'** and **9da'** showed only weak antiproliferative effects in both experimental approaches. Similarly, highly potent antimitotic 4,5-diaryl-1,2,3-triazoles (**14ad'**, **14bd'**, and **14cd'**) together with 1,5-diaryl-1,2,3-triazole **10bd'** showed significant cytotoxicity against human cancer cells. Notably, GI_{50} values for the most potent triazoles **14ad'** and **14bd'** were less than 10 nM for 50 and 10 tumor cell lines, respectively, of the 60 tested (Table 2). It should be pointed out that newly synthesized compounds **14ad'** and **14bd'**

significantly affected growth of several cancer cells otherwise insensitive to CA4. These included colon cancer HT-29, ovarian cancer OVCAR-5, renal cancer 786-0 and TK-10 cell lines (Table 2). Similar to the sea urchin embryo assay results, diaryltriazole **14bd'** with the C–C geometry was more potent than its N–C regioisomer **10bd'**. As anticipated from the sea urchin embryo tests, tetramethoxy-substituted derivative (**14cd'**) was less potent than the respective trimethoxy analogue in the cell based assay as well.

To the best of our knowledge, there is a single report dealing with the biological evaluation of 4,5-diaryl-1,2,3-triazoles (C–C geometry). According to the published data, cytotoxicity of the combretastatin analogue substituted with 3,4,5-trimethoxyphenyl- (ring A) and 4-aminophenyl- (ring B) groups was lower than expected with the IC_{50} value of 56 μM for murine B6 melanoma cells.[29] This observation further emphasizes the importance of *p*-OCH_3 substitution in the ring B. According to previous SAR studies of combretastatin derivatives,[15] the removal of *p*-OCH_3 or its replacement with OH, Cl, Br, NO_2, and OAc functionalities reduced the cytotoxicity. Moreover, the introduction of *p*-NO_2 group resulted in inactive molecule.

Insert Table 2.

It should be noted that compounds **10bd'**, **14ad'**, **14bd'**, and **14cd'** showed higher cytotoxicity against multi-drug resistant human ovarian cells MDR NCI/ADR-RES overexpressing P-glycoprotein than against the parent cell line OVCAR-8 (Table 2). This observation suggests that the selected molecules were not substrates of this transmembrane transporter and are not likely to be effluxed.

1,5-Diaryl-1,2,3-triazole **10ad'** that altered sea urchin embryo development at 0.02 μM by microtubule destabilizing mode of action, was reported to inhibit polymerization of purified tubulin.[31] This compound displayed potent antiproliferative activity against human cancer cells with IC_{50} of 0.027 μM for K562 human leukemia cells[31] and IC_{50} of 0.020–0.053 μM for 4 human cancer cell lines including multi-drug resistant cells.[39] Similar to the SAR results from the sea urchin embryo assay, the

respective regioisomer **10da'** was less active with IC_{50} of 4 μM for K562 human leukemia cells[31] and IC_{50} > 1 μM for SH-SY5Y human neuroblastoma cells.[30]

2.2.3. Induction of apoptosis in Jurkat and multi-drug resistant Jurkat A4 cells

A summary of data on cytotoxic activity of **10ad'** against Jurkat human leukemia T-cells and its multi-drug resistant subclone Jurkat A4 is presented in Figure 2. CA4P was used as a reference compound. In Jurkat cells, **10ad'** showed cytotoxicity similar to that of CA4P with EC_{50} of 30 nM and 15 nM, respectively. Notably, **10ad'** had similar activity in the sea urchin embryo assay (cleavage alteration EC = 20 nM, Table 1). In contrast, both **10ad'** and CA4P were much less toxic in Jurkat/A4 cells with multi-drug resistant phenotype exhibiting the death fraction less than 20 % even at concentration of 1 μM. Nevertheless, the delayed death of Jurkat/A4 cells was observed after two-hour exposure to **10ad'** followed by seven days cultivation in drug-free medium (data not shown). Based on these cytotoxicity results, agents **10ad'** and CA4P were subsequently used at their EC_{50} concentrations in Jurkat cells, whereas Jurkat/A4 cells were exposed to 10-times higher concentrations for both compounds.

Insert Figures 2 and 3.

We next assessed the effect of compound **10ad'** on the cell cycle distribution. It was found that **10ad'** induced cell cycle arrest at G_2/M phase with concomitant decrease of G_0/G_1 phase in both Jurkat and Jurkat/A4 cells, similarly to CA4P (Fig. 3). However, the effective concentrations of both **10ad'** and CA4P in Jurkat/A4 cells were 10-times higher. Our results suggested that **10ad'** exhibited antimitotic activity comparable with that of CA4P in both parental and multi-drug resistant leukemia cells.

Research over the last two decades has provided convincing evidence that the cell cycle arrest at G_2/M phase induced by CA4 and its derivatives eventually leads to cell death *via* apoptosis and mitotic catastrophe.[20,55] To examine possible mechanism(s) of cell death caused by **10ad'**, we analyzed morphological changes in Jurkat and Jurkat/A4 cells after exposure to this compound. It was discovered

that both **10ad'** and CA4P caused marked alterations in chromosome segregation. Namely, we observed formation of micronuclei and small cell fragments containing unequally segregated chromosomes enclosed by cell membrane (Fig. 4). Such nuclear alterations could be considered as indicators of mitotic catastrophe.[56] In addition, detection of condensed and fragmented nuclei typical for compounds that affect mitotic spindle organization was suggestive of the early stages of apoptosis. In Jurkat cells, the morphological features of apoptosis became more evident with the increase of concentration for both molecules (data not shown).

To gain insight into the mechanisms underlying the cytotoxic effect of **10ad'**, apoptogenic activity of this compound was examined. CA4P was used as a reference molecule. As shown in Figure 5, sub-G1 population became evident in Jurkat cells treated with **10ad'** (30 nM, 48 h) but not in multi-drug resistant Jurkat/A4 cells even at 10-times higher concentration of the compound (300 nM). Similar results were obtained with CA4P in both cell lines.

Insert Figures 4 and 5.

Caspases are known to play a pivotal role in both initiation and execution of apoptotic cell death.[57,58] Caspase-9 is a major initiator caspase for intrinsic (receptor-independent) apoptotic signaling pathway. Caspase-2 is unique in this class as it combines the properties of both initiator and effector caspases. On the one hand, its structure and activation mode resemble those of caspase-9. Caspase-9 organization features a long prodomain containing a CARD sequence and procaspase autoprocessing. On the other hand, its substrate specificity is similar to that of effector caspases-3 and -7. Both intrinsic and extrinsic (receptor-mediated) apoptotic signaling pathways lead to activation of the effector caspase-3, which is the main protease that degrades the cell.

To assess the role of caspases as apoptosis markers in cell death caused by **10ad'**, Jurkat and Jurkat/A4 cells were pretreated with the pancaspase peptide inhibitor z-VAD-fmk for 3 h followed by the addition of **10ad'**. Figure 6 demonstrates that pretreatment with z-VAD-fmk decreased the percentage of hypodiploid Jurkat cells, but not Jurkat/A4 cells exposed to **10ad'** or CA4P. The

involvement of initiator caspases in **10ad'**- or CA4P-induced apoptosis was further examined by Western blot analysis (Fig. 7A). In Jurkat cells, the band corresponding to the active form of caspase-9 was evident after 48 h exposure to either **10ad'** or CA4P. The involvement of caspase-9 in cell death induced by **10ad'** has been also shown recently in PC12 rat pheochromocytoma cells.[35] The active form of caspase-2 was expressed both in 24 h and 48 h samples. The band intensity was slightly increased for samples with longer exposure time. Activation of neither caspase-9 nor caspase-2 was observed in Jurkat/A4 cells treated with either **10ad'** or CA4P (Fig. 7A). Improtantly, caspase-2 activation is a prerequisite of mitotic catastrophe,[56,59] suggesting possible contribution of mitotic catastrophe in **10ad'**-induced death of Jurkat cells.

Insert Figures 6 and 7.

Proteins of IAP and Bcl-2 families are known to be the critical regulators of apoptosis. Particularly, X-linked inhibitor of apoptosis expression (XIAP) and Bcl-2 antiapoptotic proteins that block cell death machinery are involved in the development of drug resistance of tumor cells. As reported previously, XIAP undergoes cleavage by active caspase-3.[60] Therefore we analyzed the effect of compound **10ad'** on XIAP and Bcl-2 expression in Jurkat leukemia cells. It was found that **10ad'** as well as CA4P after 24 h treatment caused the reduction of XIAP band density in Jurkat cell line but not in the multi-drug resistant counterpart. Similarly, we reported previously the decreased XIAP expression upon etoposide-triggered apoptosis in Jurkat but not in Jurkat/A4 cells.[61] In contrast to XIAP, no detectable changes in the levels of antiapoptotic Bcl-2 expression in either Jurkat or Jurkat/A4 cells have been found (Fig. 7B).

Next, to explore the role of effector caspase-3 in **10ad'**- and CA4P-induced apoptosis, flow cytometry and FITC-conjugated active caspase-3 MoAb were used. As evidenced from Figure 8, the percentage of cells with active form of caspase-3 increased in a time-dependent manner in Jurkat but not Jurkat/A4 cells exposed to both CA4P and **10ad'**. We examined also whether **10ad'**-induced apoptosis was associated with cleavage of caspase substrate PARP-1. Figure 8 demonstrates that

apoptosis induction in Jurkat cells at 30 nM of **10ad'** was accompanied by PARP-1 processing, as evident by flow cytometric analysis with MoAb that specifically recognizes the cleaved form of PARP-1. In contrast, no PARP-1 cleavage was observed in Jurkat/A4 cells exposed to **10ad'** at 10-times higher concentration.

Taken together, our results provide evidence that both **10ad'** and CA4P are potent apoptosis inducers in Jurkat cells. Accumulation of Jurkat cells in G_2/M phase in the presence of **10ad'** was associated with the increased number of hypodiploid apoptotic sub-G1 cells. Caspase-9 and -2 activation caused by **10ad'** or CA4P is in agreement with the recent data[62,63] that point to the role of these caspases in the cell death induced by different CA4 derivatives. Moreover, the involvement of caspase-2 in apoptosis induced by both microtubule-destabilizing and microtubule-stabilizing agents of other chemical classes has been reported.[64] The fragmentation of PARP-1 in **10ad'**- treated Jurkat cells served as another proof of caspase-dependent cytotoxicity caused by this molecule. The observed decrease of XIAP expression in Jurkat cells after treatment with **10ad'** or CA4P correlates well with the literature data suggesting that apoptotic cell death induced by CA4 and/or its analogues coincided with the downregulation of XIAP protein.[63,65] The expression of antiapoptotic Bcl-2 protein was unaffected by **10ad'** or CA4P treatment, similar to the reported lack of effect of CA4P on Bcl-2 expression levels in WSU-CLL cells.[66] Thus, the regulation of XIAP but not Bcl-2 expression may be involved in **10ad'**- and CA4P-induced apoptosis in Jurkat cells. It should be noted that in addition to caspase-dependent apoptosis caused by **10ad'** and CA4P an alternative form(s) of cell death could be operative, since the suppression of apoptosis by pancaspase inhibitor z-VAD-fmk was incomplete. Specific morphological alterations as well as caspase-2 involvement suggested that mitotic catastrophe could represent one of nonapoptotic routes of cell death in Jurkat cells exposed to **10ad'**.

Jurkat/A4 cells with multi-drug resistant phenotype were characterized by altered components of cell death machinery.[61] Although both **10ad'** and CA4P induced mitotic arrest in Jurkat/A4 cells followed by delayed death, we could not observe any increase in the hypodiploid cell fraction,

activation of caspase-2, -3, and -9, downregulation of XIAP expression, and induction of PARP-1 cleavage, all characteristic features of apoptosis. The identification of cell death mode in Jurkat/A4 cells treated by microtubule destabilizing compound **10ad'** requires further investigations using a diverse panel of biochemical and functional assays.[67]

3. Conclusions

Based on results of the *in vivo* sea urchin embryo assay, cytotoxicity panel of 60 human tumor cell lines, and Jurkat cells activity data, we identified 1,5-diaryl-1,2,3-triazole derivatives **10ad'** and **10bd'** and 4,5-diaryl-1,2,3-triazole derivatives **14ad'** and **14bd'** featuring 3,4,5-trimethoxyphenyl and 3,4-methylenedioxy-5-methoxyphenyl ring A, respectively, as potent antimitotic microtubule destabilizing agents. At low nanomolar concentrations these compounds blocked proliferation of multiple human tumor cell lines including multi-drug resistant P-glycoprotein overexpressing cells. Triazoles **14ad'** and **14bd'** (C–C geometry) were found to be considerably more active than the respective 1,5-diaryl-1,2,3-triazoles **10ad'** and **10bd'** (N–C geometry). The mechanism of cell death under exposure of triazoles has been investigated with compound **10ad'** in human T-leukemia Jurkat cells. This molecule induced G_2/M cell cycle arrest and apoptosis *via* caspase 2/3/9 activation and downregulation of the antiapoptotic protein XIAP. In addition to apoptosis, micronucleated cell formation together with caspase-2 activation indicated possible involvement of mitotic catastrophe. In multi-drug resistant Jurkat/A4 cells, **10ad'** also exhibited lethal effect by unknown mechanism. Considering these encouraging data from phenotypic and mechanistic studies, **10ad'**, **10bd'**, **14ad'**, and **14bd'** may prove to be lead candidates for further *in vivo* studies to assess its potential as an anti-tumor agents.

4. Experimental section

4.1. Chemistry

NMR spectra were collected on a Bruker DR-500 instrument [working frequencies of 500.13 MHz (^{1}H) and 75.47 (^{13}C)]. Mass spectra were obtained on a Finnigan MAT/INCOS 50 instrument (70

eV) using direct probe injection. Elemental analysis was accomplished with the automated Perkin-Elmer 2400 CHN microanalyzer. The compound purity has been determined by NMR, HPLC, and elemental analyses. Purity of targeted compounds was determined to be ≥ 95%.

Alkyl 1,2,3-triazole-4-carboxylates **7** and 1,2,3-triazole-4-carbonitriles **5** were prepared from arylazides and β-ketoesters (β-ketonitriles) as previously described.[52]

4.1.1. General procedure for the synthesis of arylamines (3, 9) by Curtius rearrangement

A suspension of the acid (20 mmol) in $SOCl_2$ (5 mL) was refluxed for 2.5 h, excess of $SOCl_2$ was thoroughly removed with abs. benzene (2 × 4 mL) affording acid chloride. After dilution with acetone (88 mL), a solution of NaN_3 (3.25 g, 50 mmol) in water (11 mL) was added dropwise at 0– -2 °C for 20 min with stirring. The reaction mixture was further stirred at 0 °C for 1 h, warmed to rt, then the solvent was thoroughly removed at 30–35 °C *in vacuo*. The residue was diluted with water (30 mL), and targeted acyl azide was extracted with CH_2Cl_2 (3 × 50 mL). The combined extracts were washed with water (3 × 50 mL), dried by filtration through cotton plug, the solvent was removed, and the residue was thoroughly dried over P_2O_5 at 30 °C. The resulting acyl azide (yield 95–96%) was suspended in abs. EtOH (15 mL), warmed slowly to 85–90 °C with stirring (N_2 evolution was observed), and refluxed for 5 h affording urethane (yield ca. 94%) solution. The solvent was removed *in vacuo*, then aqueous NaOH (1N, 60 mL) and EtOH (8 mL) were added. The mixture was refluxed for 8 h, EtOH was removed, and the residue was extracted with CH_2Cl_2 (3 × 50 mL). The combined extract was washed with water (3 × 50 mL), dried, and the solvent was removed. The targeted arylamines **3** or 1,2,3-triazolamines **9** were washed with MeOH.

4.1.1.1. Intermediate ethyl 7-methoxy-1,3-benzodioxol-5-yl-carbamate. White solid, yield 100%, mp 71–73 °C. ^{1}H NMR (DMSO-d_6): δ 1.22 (t, J = 7.1 Hz, 3H, CH_3CH_2O), 3.77 (s, 3H, OCH_3), 4.10 (k, J = 7.1 Hz, 2H, OCH_2CH_3), 5.92 (s, 2H, OCH_2O), 6.76 (d, J = 1.9 Hz, 1H, H-4), 6.78 (d, J = 1.9 Hz, 1H, H-

6), 9.47 (s, 1H, NH). EIMS *m/z* 239 $[M]^+$ (84), 211 (32), 193 (69), 180 (15), 167 (41), 166 (100), 148 (7), 136 (8), 124 (17), 124 (11), 122 (10), 108 (9), 94 (8), 79 (23), 68 (11), 53 (19).

4.1.1.2. 7-Methoxy-1,3-benzodioxol-5-amine (3b). White solid, yield 57% (starting from benzoic acid), mp 85–86 °C (H_2O) (lit. 85–86 °C).[68] ^{1}H NMR (DMSO-d_6): δ3.72 (s, 3H, OCH_3), 4.80 (s, 2H, NH_2), 5.75 (s, 2H, OCH_2O), 5.83 (d, J = 1.9 Hz, 1H, H-6), 5.86 (d, J = 1.9 Hz, 1H, H-4). EIMS *m/z* 167 $[M]^+$ (100), 152 (1), 138 (3), 124 (17), 122 (12), 110 (8), 95 (14), 80 (51), 68 (15), 65 (6), 52 (21). Anal. Calcd for $C_8H_9NO_3$: C, 57.48; H, 5.43; N, 8.38. Found: C, 57.65; H, 5.49; N, 8.23.

4.1.1.3. Intermediate ethyl 4,7-dimethoxy-1,3-benzodioxol-5-yl-carbamate. White solid, yield 100%, mp 85–90 °C. ^{1}H NMR (DMSO-d_6): δ1.22 (t, J = 7.1 Hz, 3H, CH_3CH_2O), 3.75 (s, 3H, OCH_3-7), 3.78 (s, 3H, OCH_3-4), 4.08 (k, J = 7.1 Hz, 2H, OCH_2CH_3), 5.98 (s, 2H, OCH_2O), 6.83 (s, 1H, H-6), 8.49 (s, 1H, NH). EIMS *m/z* 269 $[M]^+$ (100), 254 (15), 224 (4), 223 (18), 208 (29), 196 (17), 182 (53), 166 (18), 152 (11), 136 (12), 124 (13), 110 (17), 95 (10), 93 (10), 82 (11), 80 (16), 68 (32), 65 (25), 53 (34).

4.1.1.4. 5-Amino-4,7-dimethoxy-1,3-benzodioxole (3c). White solid, yield 86% (starting from benzoic acid), mp 70–71 °C (lit. 70–72 °C).[69] ^{1}H NMR (DMSO-d_6): δ3.70 (s, 3H, OCH_3-7), 3.72 (s, 3H, OCH_3-4), 4.56 (s, 2H, NH_2), 5.81 (s, 2H, OCH_2O), 5.94 (s, 1H, H-6). EIMS *m/z* 197 $[M]^+$ (94), 182 (100), 166 (4), 154 (11), 152 (19), 137 (10), 124 (34), 109 (10), 96 (16), 94 (9), 92 (7), 81 (19), 68 (32), 65 (16), 53 (35). Anal. Calcd for $C_9H_{11}NO_4$: C, 54.82; H, 5.62; N, 7.10. Found: C, 54.88; H, 5.69; N, 7.17.

4.1.2. General procedure for the synthesis of arylazides (4)

Prepared according to published procedure[51] and used without further purification.

4.1.2.1. 6-Azido-4-methoxy-1,3-benzodioxole (4b). White solid, yield 85%, mp 70–72 °C. ^{1}H NMR (DMSO-d_6): δ3.83 (s, 3H, OCH_3-4), 6.01 (s, 2H, OCH_2O), 6.37 (d, J = 1.9 Hz, 1H, H-5), 6.47 (d, J = 1.9 Hz, 1H, H-7). EIMS *m/z* 193 $[M]^+$ (12), 165 (44), 150 (14), 107 (6), 94 (5), 92 (7), 77 (15), 68 (12), 64 (19), 55 (57), 53 (100). Anal. Calcd for $C_8H_7N_3O_3$: C, 49.74; H, 3.65; N, 21.75. Found: C, 49.64; H, 3.61; N, 21.84.

4.1.2.2. 5-Azido-4,7-dimethoxy-1,3-benzodioxole (4c). White solid, yield 62%, mp 68–70 °C. ^{1}H NMR (DMSO-d_6): δ3.77 (s, 3H, OCH_3-4), 3.83 (s, 3H, OCH_3-7), 6.03 (s, 2H, OCH_2O), 6.32 (s, 1H, H-6). EIMS *m/z* 223 $[M]^+$ (26), 195 (63), 194 (27), 180 (41), 152 (12), 150 (27), 138 (10), 136 (10), 124 (47), 122 (31), 96 (56), 94 (43), 83 (69), 82 (44), 79 (42), 78 (18), 68 (38), 67 (38), 64 (34), 53 (100). Anal. Calcd for $C_9H_9N_3O_4$: C, 48.43; H, 4.06; N, 18.83. Found: C, 48.37; H, 4.03; N, 18.89.

4.1.3. General procedure for the synthesis of carbonitriles (5)

Prepared according to published procedure.[52]

4.1.3.1. 1,5-Bis(3,4,5-trimethoxyphenyl)-1,2,3-triazole-4-carbonitrile (5aa'). White solid, yield 79%, mp 184–185 °C (EtOH). ^{1}H NMR (DMSO-d_6): δ3.66 (s, 6H, OCH_3-3',5'), 3.70 (s, 6H, OCH_3-4', 4"), 3.71 (s, 6H, OCH_3-3",5"), 6.81 (s, 2H, H-2',6'), 6.93 (s, 2H, H-2",6"). EIMS *m/z* 426 $[M]^+$ (44), 398 (27), 384 (23), 383 (100), 367 (10), 325 (9), 231 (7), 152 (7), 137 (11), 122 (6), 120 (6), 109 (14), 107 (5), 104 (6), 92 (6), 88 (6), 81 (17), 77 (10). Anal. Calcd for $C_{21}H_{22}N_4O_6$: C, 59.15; H, 5.20; N, 13.14. Found: C, 59.29; H, 5.28; N, 13.01.

4.1.3.2. 5-(4-Methoxyphenyl)-1-(3,4,5-trimethoxyphenyl)-1,2,3-triazole-4-carbonitrile (5ad'). White solid, yield 81%, mp 145–146 °C (EtOH). ^{1}H NMR (DMSO-d_6): δ3.67 (s, 6H, OCH_3-3',5'), 3.71 (s, 3H, OCH_3-4'), 3.79 (s, 3H, OCH_3-4"), 6.87 (s, 2H, H-2',6'), 7.08 (d, J = 8.5 Hz, 2H, H-3",5"), 7.40 (d, J = 8.5 Hz, 2H, H-2",6"). EIMS *m/z* 366 $[M]^+$ (30), 340 (1), 338 (45), 323 (100), 307 (31), 295 (10), 292 (5), 280 (25), 265 (32), 249 (10), 237 (23), 209 (10), 194 (8), 178 (8), 171 (94), 152 (17), 145 (92), 139 (10), 137 (31), 133 (10), 128 (15), 122 (15), 116 (34), 114 (33), 109 (46), 107 (17), 102 (20), 92 (16), 89 (21), 81 (56), 77 (33), 76 (34), 66 (97). Anal. Calcd for $C_{19}H_{18}N_4O_4$: C, 62.29; H, 4.95; N, 15.29. Found: C, 62.21; H, 4.88; N, 15.35.

4.1.3.3. 1-(4-Methoxyphenyl)-5-(3,4,5-trimethoxyphenyl)-1,2,3-triazole-4-carbonitrile (5da'). White solid, yield 84%, mp 126–128 °C (EtOH). ^{1}H NMR (DMSO-d_6): δ3.64 (s, 6H, OCH_3-3",5"), 3.70 (s, 3H, OCH_3-4"), 3.81 (s, 3H, OCH_3-4'), 6.75 (s, 2H, H-2",6"), 7.11 (d, J = 8.9 Hz, 2H, H-3',5'), 7.46 (d, J = 8.9 Hz, 2H, H-2',6'). EIMS *m/z* 366 $[M]^+$ (34), 338 (10), 324 (20), 323 (100), 295 (10), 280

(6), 265 (11), 263 (5), 251 (6), 237 (8), 209 (15), 194 (8), 171 (11), 166 (6), 144 (7), 139 (5), 132 (5), 104 (15), 102 (11), 92 (44), 88 (17), 77 (47), 64 (34). Anal. Calcd for $C_{19}H_{18}N_4O_4$: C, 62.29; H, 4.95; N, 15.29. Found: C, 62.32; H, 4.99; N, 15.34.

4.1.3.4. 1,5-Bis(4-methoxyphenyl)-1,2,3-triazole-4-carbonitrile (5dd'). White solid, yield 75%, mp 125–126 °C (EtOH). ^{1}H NMR (DMSO-d_6): δ 3.79 (s, 3H, OCH_3-4"), 3.81 (s, 3H, OCH_3-4'), 7.06 (d, J = 8.8 Hz, 2H, H-3",5"), 7.08 (d, J = 8.9 Hz, 2H, H-3',5'), 7.34 (d, J = 8.8 Hz, 2H, H-2",6"), 7.42 (d, J = 8.9 Hz, 2H, H-2',6'). EIMS *m/z* 306 $[M]^+$ (23), 291 (1), 278 (62), 264 (17), 263 (100), 235 (34), 220 (14), 192 (23), 171 (35), 164 (7), 145 (82), 130 (13), 128 (10), 116 (33), 114 (30), 107 (12), 102 (27), 92 (92), 90 (29), 88 (19), 77 (97). Anal. Calcd for $C_{17}H_{14}N_4O_2$: C, 66.66; H, 4.61; N, 18.29. Found: C, 66.73; H, 4.66; N, 18.21.

4.1.3.5. 1-(4-Methoxyphenyl)-5-(3-methoxyphenyl)-1,2,3-triazole-4-carbonitrile (5de'). White solid, yield 73%, mp 90–92 °C (EtOH). ^{1}H NMR (DMSO-d_6): δ 3.69 (s, 3H, OCH_3-4'), 3.81 (s, 3H, OCH_3-3"), 6.97 (d, J = 7.7 Hz, 1H, H-4"), 7.00 (d, J = 2.4 Hz, 1H, H-2"), 7.08 (d, J = 8.9 Hz, 2H, H-3',5'), 7.10 (dd, J = 7.7, 2.4 Hz, 1H, H-6"), 7.42 (t, J = 7.7 Hz, 1H, H-5"), 7.42 (d, J = 8.9 Hz, 2H, H-2',6'). EIMS *m/z* 306 $[M]^+$ (45), 278 (100), 263 (100), 248 (9), 247 (7), 235 (98), 232 (12), 220 (22), 192 (44), 171 (10), 164 (10), 139 (11), 130 (11), 128 (11), 116 (25), 114 (32), 102 (27), 92 (81), 88 (16), 77 (68), 64 (78). Anal. Calcd for $C_{17}H_{14}N_4O_2$: C, 66.66; H, 4.61; N, 18.29. Found: C, 66.76; H, 4.65; N, 18.20.

4.1.3.6. 1-(3-Chlorophenyl)-5-(3,4,5-trimethoxyphenyl)-1,2,3-triazole-4-carbonitrile (5fa'). White solid, yield 78%, mp 130–131 °C (EtOH). ^{1}H NMR (DMSO-d_6): δ 3.64 (s, 6H, OCH_3-3",5"), 3.71 (s, 3H, OCH_3-4"), 6.77 (s, 2H, H-2",6"), 7.48 (d, J = 7.8 Hz, 1H, H-4'), 7.60 (t, J = 7.8 Hz, 1H, H-5'), 7.70 (d, J = 7.8 Hz, 1H, H-6'), 7.76 (s, 1H, H-2'). EIMS *m/z* 372 $[M+2]^+$ (14), 370 $[M]^+$ (41), 329 (30), 327 (88), 299 (15), 283 (5), 269 (11), 255 (7), 231 (9), 215 (8), 213 (21), 203 (6), 201 (7), 178 (9), 171 (10), 162 (6), 151 (6), 145 (8), 144 (9), 113 (30), 111 (82), 104 (22), 102 (18), 100 (10), 88 (33), 77 (11), 76 (38), 75 (100). Anal. Calcd for $C_{18}H_{15}ClN_4O_3$: C, 58.31; H, 4.08; Cl, 9.56; N, 15.11. Found: C, 58.24; H, 4.03; Cl, 9.62; N, 15.15.

4.1.3.7. 1-(3-Chlorophenyl)-5-(3-methoxyphenyl)-1,2,3-triazole-4-carbonitrile (5fe'). White solid, yield 72%, mp 100–102 °C (EtOH). ^{1}H NMR (DMSO-d_6): δ 3.70 (s, 3H, OCH_3-3''), 6.99 (d, J = 8.9 Hz, 1H, H-4''), 7.02 (s, 1H, H-2''), 7.14 (d, J = 8.9 Hz, 1H, H-6''), 7.45 (t, J = 8.9 Hz, 1H, H-5''), 7.47 (d, J = 8.0 Hz, 1H, H-4'), 7.59 (t, J = 8.0 Hz, 1H, H-5'), 7.69 (d, J = 8.0 Hz, 1H, H-6'), 7.72 (s, 1H, H-2'). EIMS *m/z* 312 $[M+2]^+$ (10), 310 $[M]^+$ (36), 284 (23), 282 (74), 267 (6), 247 (14), 241 (13), 239 (39), 232 (10), 203 (9), 171 (12), 128 (10), 116 (23), 114 (41), 113 (25), 111 (69), 102 (18), 101 (12), 90 (15), 88 (15), 87 (11), 76 (31), 75 (100). Anal. Calcd for $C_{16}H_{11}ClN_4O$: C, 61.84; H, 3.57; Cl, 11.41; N, 18.03. Found: C, 61.76; H, 3.52; Cl, 11.44; N, 18.07.

4.1.4. General procedure for the synthesis of 1,5-diaryl-1,2,3-triazole-4-carboxamides (6)

The corresponding 1,2,3-triazole-4-carbonitrile (2 mmol) was dissolved in conc. H_2SO_4 (1 mL) and kept for 10 h. The reaction mixture was poured onto ice (10 g). The resulting precipitate was filtered off and recrystallized from 50% aqueous MeOH.

4.1.4.1. 1,5-Bis(3,4,5-trimethoxyphenyl)-1,2,3-triazole-4-carboxamide (6aa'). White solid, yield 66%, mp 199–200 °C. ^{1}H NMR (DMSO-d_6): δ 3.62 (s, 6H, OCH_3-3'',5''), 3.67 (s, 12H, OCH_3-3',4',5', 4''), 6.73 (s, 2H, H-2',6'), 6.77 (s, 2H, H-2'',6''), 7.50 and 7.93 (s, 2H, $CONH_2$). EIMS *m/z* 444 $[M]^+$ (68), 416 (15), 402 (9), 401 (46), 373 (33), 358 (35), 342 (8), 327 (5), 315 (8), 300 (10), 284 (6), 356 (5), 218 (5), 209 (40), 207 (13), 206 (14), 193 (70), 179 (11), 168 (82), 165 (24), 152 (21), 150 (18), 148 (15), 145 (12), 140 (19), 137 (134), 135 (16), 134 (15), 133 (12), 122 (22), 120 (18), 119 (12), 109 (42), 107 (22), 104 (15), 93 (21), 92 (22), 81 (49), 77 (36), 66 (63), 53 (40), 44 (100). Anal. Calcd for $C_{21}H_{24}N_4O_7$: C, 56.75; H, 5.44; N, 12.61. Found: C, 59.86; H, 5.49; N, 12.54.

4.1.4.2. 5-(4-Methoxyphenyl)-1-(3,4,5-trimethoxyphenyl)-1,2,3-triazole-4-carboxamide (6ad'). White solid, yield 69%, mp 150–151 °C. ^{1}H NMR (DMSO-d_6): δ 3.64 (s, 6H, OCH_3-3',5'), 3.67 (s, 3H, OCH_3-4'), 3.76 (s, 3H, OCH_3-4''), 6.70 (s, 2H, H-2',6'), 6.93 (d, J = 8.6 Hz, 2H, H-3'',5''), 7.29 (d, J = 8.6 Hz, 2H, H-2'',6''), 7.45 and 7.88 (s, 2H, $CONH_2$). EIMS *m/z* 384 $[M]^+$ (30), 356 (10), 341 (39), 313 (30), 298 (32), 283 (6), 270 (6), 255 (16), 240 (9), 212 (6), 209 (8), 194 (29), 168 (21), 166 (8), 152 (80,

146 (26), 140 (11), 137 (15), 134 (26), 119 (15), 109 (25), 100 (11), 91 (21), 81 (27), 77 (25), 66 (44), 44 (100). Anal. Calcd for $C_{19}H_{20}N_4O_5$: C, 59.37; H, 5.24; N, 14.58. Found: C, 59.46; H, 5.28; N, 14.52.

4.1.5. General procedure for the synthesis of 1,5-diaryl-1,2,3-triazole-4-carboxylates (7)

Prepared according to published procedure.[52]

4.1.5.1. Methyl 5-(4-methoxyphenyl)-1-(3,4,5-trimethoxyphenyl)-1,2,3-triazole-4-carboxylate (7ad'). White solid, yield 93%, mp 145–147 °C. ^{1}H NMR (DMSO-d_6): δ3.64 (s, 6H, OCH_3-3',5'), 3.68 (s, 3H, OCH_3-4'), 3.76 (s, 3H, OCH_3-4"), 3.77 (s, 3H, CO_2CH_3), 6.73 (s, 2H, H-2',6'), 6.97 (d, J = 8.8 Hz, 2H, H-3",5"), 7.32 (d, J = 8.8 Hz, 2H, H-2",6"). EIMS *m/z* 399 $[M]^+$ (42), 371 (60), 356 (100), 340 (11), 328 (24), 312 (28), 298 (13), 297 (14), 285 (11), 282 (20), 270 (18), 254 (29), 209 (10), 204 (10), 195 (35), 194 (21), 170 (10), 166 (11), 156 (11), 152 (14), 146 (14), 140 (10), 137 (19), 135 (45), 121 (20), 119 (23), 109 (29), 107 (17), 102 (11), 92 (18), 81 (42), 77 (39). Anal. Calcd for $C_{20}H_{21}N_3O_6$: C, 60.14; H, 5.30; N, 10.52. Found: C, 60.22; H, 5.34; N, 10.48.

4.1.5.2. Ethyl 1-(4-methoxyphenyl)-5-(3,4,5-trimethoxyphenyl)-1,2,3-triazole-4-carboxylate (7a'd). White solid, yield 78%, mp 145–147 °C (EtOH). ^{1}H NMR (DMSO-d_6): δ1.17 (t, J = 7.1 Hz, 3H, CH_3CH_2), 3.63 (s, 6H, OCH_3-3",5"), 3.67 (s, 3H, OCH_3-4"), 3.78 (s, 3H, OCH_3-4'), 4.24 (k, J = 7.1 Hz, 2H, OCH_2CH_3), 6.71 (s, 2H, H-2",6"), 7.03 (d, J = 8.9 Hz, 2H, H-3',5'), 7.37 (d, J = 8.9 Hz, 2H, H-2',6'). EIMS *m/z* 413 $[M]^+$ (25), 385 (16), 370 (68), 312 (15), 282 (11), 254 (12), 239 (8), 224 (13), 195 (20), 193 (10), 183 (15), 179 (14), 170 (11), 165 (16), 163 (12), 150 (53), 135 (28), 127 (9), 121 (14), 107 (24), 104 (17), 92 (72), 90 (16), 77 (100). Anal. Calcd for $C_{21}H_{23}N_3O_6$: C, 61.01; H, 5.61; N, 10.16. Found: C, 61.14; H, 5.69; N, 10.01.

4.1.5.3. Ethyl 1-(3-chlorophenyl)-5-phenyl-1,2,3-triazole-4-carboxylate (7fg'). White solid, yield 85%, mp 135–137 °C. ^{1}H NMR (DMSO-d_6): δ1.14 (t, J = 7.1 Hz, 3H, CH_3CH_2O), 4.22 (k, J = 7.1 Hz, 2H, OCH_2CH_3), 7.35 (dd, J = 8.1, 2.0 Hz, 1H, H-4'), 7.39 (d, J = 6.5 Hz, 2H, H-2",6"), 7.41 (t, J = 6.5 Hz, 2H, H-3", 5"), 7.44 (t, J = 6.5 Hz, 1H, H-4"), 7.49 (t, J = 8.1 Hz, 1H, H-5'), 7.57 (t, J = 2.0 Hz, 1H, H-2'), 7.58 (dd, J = 8.1, 2.0 Hz, 1H, H-6'). EIMS *m/z* 329 $[M+2]^+$ (12), 327 $[M]^+$ (34), 302 (4), 300 (2),

299 (12), 271 (5), 255 (8), 229 (18), 227 (27), 226 (36), 214 (33), 208 (11), 165 (12), 154 (16), 145 (47), 129 (14), 118 (61), 113 (12), 111 (30), 105 (33), 89 (10), 77 (13), 75 (28). Anal. Calcd for $C_{17}H_{14}ClN_3O_2$: C, 62.30; H, 4.31; Cl, 10.82; N, 12.82. Found: C, 62.42; H, 4.35 Cl, 10.78; N, 12.76.

4.1.5.4. Methyl 1-(7-methoxy-1,3-benzodioxol-5-yl)-5-(4-methoxyphenyl)-1*H*-1,2,3-triazole-4-carboxylate (7bd'). White solid, yield 97%, mp 165–167 °C. ^{1}H NMR (DMSO-d_6): δ3.72 (s, 3H, OCH_3-7'), 3.76 (s, 3H, OCH_3-4"), 3.78 (s, 3H, $COOCH_3$), 6.07 (s, 2H, OCH_2O), 6.68 (d, J = 1.9 Hz, 1H, H-6'), 6.77 (d, J = 1.9 Hz, 1H, H-4'), 6.96 (d, J = 8.8 Hz, 2H, H-3",5"), 7.31 (d, J = 8.8 Hz, 2H, H-2",6"). EIMS *m/z* 383 $[M]^+$ (28), 355 (64), 340 (29), 312 (18), 296 (90), 281 (19), 266 (21), 254 (12), 251 (8), 238 (7), 236 (6), 225 (12), 208 (10), 204 (14), 195 (10), 193 (98), 179 (100), 167 (10), 164 (12), 152 (31), 151 (31), 148 (31), 145 (15), 135 (69), 133 (20), 123 (32), 121 (51), 119 (85), 116 (25), 102 (23), 95 (78), 93 (39), 78 (70). Anal. Calcd for $C_{19}H_{17}N_3O_6$: C, 59.53; H, 4.47; N, 10.96. Found: C, 59.78; H, 4.49; N, 11.15

4.1.5.5. Methyl 1-(4,7-Dimethoxy-1,3-benzodioxol-5-yl)-5-(4-methoxyphenyl)-1*H*-1,2,3-triazole-4-carboxylate (7cd'). This was used without further purification.

4.1.6. General procedure for the synthesis of 1,5-diaryl-1,2,3-triazole-4-carboxylic acids (8)

A mixture of the corresponding ester (2.5 mmol) and KOH in EtOH (15%, 2.5 mL) was stirred overnight at rt, and EtOH was removed. The residue was dissolved in water (20 mL) and acidified with HCl (~18%) to pH 5–6. The resulting precipitate was filtered off and washed with water to neutral pH.

4.1.6.1. 5-(4-Methoxyphenyl)-1-(3,4,5-trimethoxyphenyl)-1,2,3-triazole-4-carboxylic acid (8ad'). White solid, yield 94%, mp 175–177 °C (decomp.). ^{1}H NMR (DMSO-d_6): δ3.64 (s, 6H, OCH_3-3',5'), 3.67 (s, 3H, OCH_3-4'), 3.79 (s, 3H, OCH_3-4"), 6.72 (s, 2H, H-2',6'), 6.96 (d, J = 8.8 Hz, 2H, H-3",5"), 7.31 (d, J = 8.8 Hz, 2H, H-2",6"), 12.97 (s, 1H, CO_2H). EIMS *m/z* 385 $[M]^+$ (1), 357 (1), 341 (10), 313 (36), 298 (100), 283 (16), 270 (10), 255 (25), 240 (22), 212 (12), 210 (35), 179 (17), 175 (22), 152 (14), 147 (78), 137 (22), 135 (21), 119 (41), 109 (34), 107 (16), 103 (11), 92 (20), 89 (15), 81 (48), 79 (20), 77 (42). Anal. Calcd for $C_{19}H_{19}N_3O_6$: C, 59.22; H, 4.97; N, 10.90. Found: C, 59.28; H, 5.01; N, 10.85.

4.1.6.2. 1-(4-Methoxyphenyl)-5-(3,4,5-trimethoxyphenyl)-1,2,3-triazole-4-carboxylic acid (8da'). White solid, yield 96%, mp 192–195 °C (decomp.). ^{1}H NMR (DMSO-d_6): δ3.62 (s, 6H, OCH_3-3",5"), 3.67 (s, 3H, OCH_3-4"), 3.78 (s, 3H, OCH_3-4'), 6.70 (s, 2H, H-2",6"), 7.03 (d, J = 8.9 Hz, 2H, H-3',5'), 7.36 (d, J = 8.9 Hz, 2H, H-2',6'), 13.02 (s, 1H, COOH). EIMS *m/z* 385 $[M]^+$ (3), 342 (12), 313 (15), 298 (100), 270 (10), 255 (11), 240 (13), 226 (11), 224 (10), 212 (11), 193 (14), 184 (18), 169 (10), 165 (22), 163 (14), 150 (25), 146 (12), 141 (16), 135 (30), 134 (18), 122 (14), 120 (13), 119 (12), 107 (27), 104 (11), 92 (76), 79 (22), 77 (75). Anal. Calcd for $C_{19}H_{19}N_3O_6$: C, 59.22; H, 4.97; N, 10.90. Found: C, 59.28; H, 5.02; N, 10.85.

4.1.6.3. 1-(3-Chlorophenyl)-5-phenyl-1,2,3-triazole-4-carboxylic acid (8fg'). White solid, yield 95%, mp 165–167 °C (decomp.). ^{1}H NMR (DMSO-d_6): δ7.33 (d, J = 8.0 Hz, 1H, H-4'), 7.38 (d, J = 7.4 Hz, 2H, H-2",6"), 7.38 (t, J = 7.4 Hz, 2H, H-3", 5"), 7.43 (t, J = 7.4 Hz, 1H, H-4"), 7.48 (t, J = 8.0 Hz, 1H, H-5'), 7.55 (s, 1H, H-2'), 7.56 (d, J = 8.0 Hz, 1H, H-6'),13.12 (s, 1H, COOH). EIMS *m/z* 301 $[M+2]^+$ (4), 299 $[M]^+$ (10), 273 (5), 271 (14), 257 (8), 255 (23), 229 (37), 227 (100), 214 (22), 208 (13), 192 (45), 190 (27), 165 (61), 163 (16), 154 (17), 150 (14), 145 (40), 124 (11), 118 (26), 117 (20), 116 (32), 113 (11), 111 (53), 105 (22), 102 (11), 90 (33), 89 (81), 76 (31), 75 (69). Anal. Calcd for $C_{15}H_{10}ClN_3O_2$: C, 60.11; H, 3.36; Cl, 11.83; N, 14.02. Found: C, 60.16; H, 3.39; Cl, 11.79; N, 13.97.

4.1.6.4. 1-(7-Methoxy-1,3-benzodioxol-5-yl)-5-(4-methoxyphenyl)-1*H*-1,2,3-triazole-4-carboxylic acid (8bd'). White solid, yield 80%, mp 196–198 °C (decomp.). ^{1}H NMR (DMSO-d_6): δ3.71 (s, 3H, OCH_3-7'), 3.77 (s, 3H, OCH_3-4"), 6.07 (s, 2H, OCH_2O), 6.67 (d, J = 1.6 Hz, 1H, H-6'), 6.75 (d, J = 1.6 Hz, 1H, H-4'), 6.95 (d, J = 8.7 Hz, 2H, H-3",5"), 7.30 (d, J = 8.7 Hz, 2H, H-2",6"), 12.95 (s, 1H, COOH). EIMS *m/z* 325 $[M-CO_2]$ (15), 297 (84), 282 (91), 226 (10), 194 (31), 164 (39), 151 (16), 148 (17), 147 (17), 146 (19), 136 (26), 119 (24), 95 (44), 93 (21), 91 (22), 78 (37), 63 (32), 50 (45), 44 (100). Anal. Calcd for $C_{18}H_{15}N_3O_6$: C, 58.54; H, 4.09; N, 11.38. Found: C, 58.56; H, 3.90; N, 11.22.

4.1.6.5. 1-(4,7-Dimethoxy-1,3-benzodioxol-5-yl)-5-(4-methoxyphenyl)-1*H*-1,2,3-triazole-4-carboxylic acid (8cd'). White solid, yield 76% (on 2 steps starting from azide **4c**), mp 189–191 °C

(decomp.). ^{1}H NMR (DMSO-d_6): δ3.46 (s, 3H, OCH_3-4'), 3.76 (s, 3H, OCH_3-4''), 3.78 (s, 3H, OCH_3-7'), 6.09 (s, 2H, OCH_2O), 6.94 (d, J = 8.7 Hz, 2H, H-3'',5''), 6.99 (s, 1H, H-6'), 7.28 (d, J = 8.7 Hz, 2H, H-2'',6''), 12.96 (s, 1H, COOH). EIMS *m/z* 355 [M-CO_2] (26), 327 (60), 312 (90), 297 (15), 281 (16), 269 (9), 254 (8), 281 (16), 269 (9), 254 (8), 252 (8), 241 (6), 224 (11), 194 (13), 166 (90), 156 (13), 147 (23), 146 (28), 135 (23), 121 (14), 119 (20), 106 (17), 95 (13), 93 (26), 91 (20), 89 (18), 77 (16), 65 (33), 63 (20), 53 (77), 44 (100). Anal. Calcd for $C_{19}H_{17}N_3O_7$: C, 57.14; H, 4.29; N, 10.52. Found: C, 56.88; H, 4.06; N, 10.84.

4.1.7. General procedure for the synthesis of 1,5-diaryl-1,2,3-triazole-4-amines (9)

1,5-Diaryl-1,2,3-triazole-4-amines **9** were prepared according to General procedure for the synthesis of arylamines **3**, **9** (see above).

4.1.7.1. 5-(4-Methoxyphenyl)-1-(3,4,5-trimethoxyphenyl)-1,2,3-triazole-4-amine (9ad'). White solid, yield 68%, mp 172–174 °C. ^{1}H NMR (DMSO-d_6): δ3.63 (s, 6H, OCH_3-3',5'), 3.68 (s, 3H, OCH_3-4'), 3.76 (s, 3H, OCH_3-4''), 4.84 (s, 2H, NH_2), 6.60 (s, 2H, H-2',6'), 6.96 (d, J = 8.8 Hz, 2H, H-3'',5''), 7.18 (d, J = 8.8 Hz, 2H, H-2'',6''). EIMS *m/z* 356 $[M]^+$ (15), 328 (77), 313 (49), 300 (15), 298 (26), 297 (83), 282 (11), 270 (12), 255 (15), 227 (11), 221 (13), 194 (31), 180 (26), 179 (23), 178 (18), 164 (12), 163 (21), 161 (20), 152 (14), 148 (11), 137 (18), 134 (100), 109 (30), 107 (13), 105 (14), 94 (19), 81 (26), 77 (39). Anal. Calcd for $C_{18}H_{20}N_4O_4$: C, 60.66; H, 5.66; N, 15.72. Found: C, 60.54; H, 5.61; N, 15.83.

4.1.7.2. 1-(4-Methoxyphenyl)-5-(3,4,5-trimethoxyphenyl)-1,2,3-triazole-4-amine (9da'). White solid, yield 65%, mp 170–172 °C. ^{1}H NMR (DMSO-d_6): δ3.61 (s, 6H, OCH_3-3'',5''), 3.65 (s, 3H, OCH_3-4''), 3.79 (s, 3H, OCH_3-4'), 4.98 (s, 2H, NH_2), 6.43 (s, 2H, H-2'',6''), 7.03 (d, J = 8.9 Hz, 2H, H-3',5'), 7.28 (d, J = 8.9 Hz, 2H, H-2',6'). EIMS *m/z* 356 $[M]^+$ (5), 328 (25), 313 (25), 300 (9), 270 (5), 239 (5), 194 (25), 180 (18), 161 (23), 135 (77), 134 (100), 120 (19), 105 (31), 92 (53), 77 (64). Anal. Calcd for $C_{18}H_{20}N_4O_4$: C, 60.66; H, 5.66; N, 15.72. Found: C, 60.88; H, 5.62; N, 15.55.

4.1.7.3. 1-(3-Chlorophenyl)-5-phenyl-1,2,3-triazole-4-amine (9fg'). White solid, yield 41%, mp 107–110 °C. ^{1}H NMR (DMSO-d_6): δ 5.05 (s, 2H, NH_2), 7.22 (d, J = 7.0 Hz, 2H, H-2",6"), 7.24 (dd, J = 7.9, 2.0 Hz, 1H, H-4'), 7.34 (t, J = 7.0 Hz, 1H, H-4"), 7.39 (t, J = 7.0 Hz, 2H, H-3", 5"), 7.45 (t, J = 2.0 Hz, 1H, H-2'), 7.48 (t, J = 7.9 Hz, 1H, H-5'), 7.53 (dd, J = 7.9, 2.0 Hz, 1H, H-6'). EIMS *m/z* 272 $[M+2]^+$ (2), 270 $[M]^+$ (8), 244 (4), 242 (14), 227 (1), 216 (7), 214 (21), 207 (100), 180 (9), 165 (17), 141 (20), 140 (29), 139 (64), 138 (74), 113 (19), 111 (59), 104 (86), 89 (19), 77 (63), 75 (81). Anal. Calcd for $C_{14}H_{11}ClN_4$: C, 62.11; H, 4.10; Cl, 13.10; N, 20.70. Found: C, 62.02; H, 4.06; Cl, 13.03; N, 20.83.

4.1.8. General procedure for the synthesis of 1,5-diaryl-1,2,3-triazoles (10)

The corresponding acid **8** (1 mmol) was heated slightly above its melting point until the gas evolution ceased (1–2 min), then cooled to yield pure 1,2,3-triazoles.

4.1.8.1. 5-(4-Methoxyphenyl)-1-(3,4,5-trimethoxyphenyl)-1,2,3-triazole (10ad'). White solid, yield 98%, mp 125–127 °C (lit.[31] 126 °C). ^{1}H NMR (DMSO-d_6): δ 3.68 (s, 6H, OCH_3-3',5'), 3.72 (s, 3H, OCH_3-4'), 3.76 (s, 3H, OCH_3-4"), 6.74 (s, 2H, H-2',6'), 6.98 (d, J = 8.8 Hz, 2H, H-3",5"), 7.27 (d, J = 8.8 Hz, 2H, H-2",6"), 8.04 (s, 1H, H-4). EIMS *m/z* 341 $[M]^+$ (68), 313 (81), 298 (100), 282 (12), 255 (30), 240 (24), 212 (23), 152 (14), 146 (63), 137 (15), 122 (11), 120 (11), 109 (23), 103 (11), 91 (26), 89 (17), 81 (31), 77 (27). Anal. Calcd for $C_{18}H_{19}N_3O_4$: C, 63.33; H, 5.61; N, 12.31. Found: C, 63.24; H, 5.58; N, 12.39.

4.1.8.2. 1-(4-Methoxyphenyl)-5-(3,4,5-trimethoxyphenyl)-1,2,3-triazole (10da'). White solid, yield 100%, mp 145–147 °C. ^{1}H NMR (DMSO-d_6): δ 3.61 (s, 6H, OCH_3-3",5"), 3.66 (s, 3H, OCH_3-4"), 3.82 (s, 3H, OCH_3-4'), 6.57 (s, 2H, H-2",6"), 7.10 (d, J = 8.8 Hz, 2H, H-3',5'), 7.38 (d, J = 8.8 Hz, 2H, H-2',6'), 8.12 (s, 1H, H-4). EIMS *m/z* 341 $[M]^+$ (33), 313 (9), 298 (100), 270 (7), 240 (9), 226 (8), 206 (5), 184 (10), 146 (7), 107 (7), 92 (25), 79 (16), 77 (31). Anal. Calcd for $C_{18}H_{19}N_3O_4$: C, 63.33; H, 5.61; N, 12.31. Found: C, 63.27; H, 5.56; N, 12.37.

4.1.8.3. 1-(7-Methoxy-1,3-benzodioxol-5-yl)-5-(4-methoxyphenyl)-1*H*-1,2,3-triazole (10bd'). White solid, yield 89%, mp 112–114 °C. ^{1}H NMR (DMSO-d_6): δ 3.76 (s, 6H, OCH_3-7',4"), 6.11 (s, 2H,

OCH_2O), 6.67 (d, *J* = 1.9 Hz, 1H, H-6'), 6.78 (d, *J* = 1.9 Hz, 1H, H-4'), 6.98 (d, *J* = 8.8 Hz, 2H, H-3",5"), 7.26 (d, *J* = 8.8 Hz, 2H, H-2",6"), 8.01 (s, 1H, H-4). EIMS *m/z* 325 $[M]^+$ (52), 297 (65), 282 (100), 254 (11), 224 (11), 151 (30), 146 (47), 120 (13), 103 (15), 95 (56), 93 (20), 91 (37), 89 (26), 78 (34), 77 (27). Anal. Calcd for $C_{17}H_{15}N_3O_4$: C, 62.76; H, 4.65; N, 12.92. Found: C, 62.83; H, 4.68; N, 12.85.

4.1.8.4. 1-(4,7-Dimethoxy-1,3-benzodioxol-5-yl)-5-(4-methoxyphenyl)-1*H*-1,2,3-triazole (10cd'). White solid, yield 76%, mp 125–127 °C. ^{1}H NMR (DMSO-d_6): δ3.39 (s, 3H, OCH_3-4'), 3.75 (s, 3H, OCH_3-4"), 3.81 (s, 3H, OCH_3-7'), 6.13 (s, 2H, OCH_2O), 6.93 (s, 1H, H-6'), 6.98 (d, *J* = 8.8 Hz, 2H, H-3",5"), 7.26 (d, *J* = 8.8 Hz, 2H, H-2",6"), 8.03 (s, 1H, H-4). EIMS *m/z* 355 $[M]^+$ (70), 327 (59), 312 (100), 297 (11), 281 (24), 269 (14), 268 (11), 252 (10), 243 (10), 182 (6), 156 (21), 146 (54), 135 (20), 121 (19), 117 (11), 106 (20), 103 (15), 95 (19), 93 (32), 91 (36), 89 (35), 77 (41). Anal. Calcd for $C_{18}H_{17}N_3O_5$: C, 60.84; H, 4.82; N, 11.83. Found: C, 60.97; H, 4.87; N, 11.73.

4.1.8.5. 1-(3-Chlorophenyl)-5-phenyl-1,2,3-triazole (10fg'). White solid, yield 99%, mp 75–77 °C. ^{1}H NMR (DMSO-d_6): δ7.32 (m, 2H, H-2",6"), 7.37 (d, *J* = 7.9 Hz, 1H, H-4'), 7.43 (m, 3H, H-3",4",5"), 7.55 (t, *J* = 7.9 Hz, 1H, H-5'), 7.61 (s, 1H, H-2'), 7.63 (d, *J* = 7.9 Hz, 1H, H-6'), 8.15 (s, 1H, H-4). EIMS *m/z* 257 $[M+2]^+$ (19), 255 $[M]^+$ (58), 229 (38), 227 (100), 192 (36), 165 (43), 116 (14), 113 (12), 111 (43), 102 (12), 90 (25), 89 (61), 76 (25), 75 (59). Anal. Calcd for $C_{14}H_{10}ClN_3$: C, 65.76; H, 3.94; Cl, 13.86; N, 16.43. Found: C, 65.68; H, 3.92; Cl, 13.79; N, 16.57.

4.1.9. General procedure for the synthesis of arylalkynes (11)

K_2CO_3 (4.15 g, 30 mmol) was added to the stirred solution of corresponding benzaldehyde (15 mmol) and 1-diazo-2-oxopropylphosphonate (3.69 g, 18 mmol) in dry methanol (55 mL) at 0°C (ice-water bath).[70] The reaction mixture was stirred overnight in ice-water bath, then methanol was evaporated, and the residue was dissolved in 15 mL of cold water. The precipitate was filtered off, washed with water, and dried *in vacuo* to yield arylalkyne as colorless crystals. The targeted arylalkynes **11** were used without further purification.

4.1.9.1. 5-Ethynyl-1,2,3-trimethoxybenzene (11a). White solid, yield 99%, mp 68–70 °C (lit.[31] 68–70 °C). ^{1}H NMR ($CDCl_3$): δ 3.03 (s, 1H, CH), 3.86 (s, 9H, 3 x OCH_3), 6.73 (s, 2H, H-4,6). EIMS *m/z* 192 $[M]^+$ (100), 177 (58), 162 (3), 149 (26), 134 (25), 119 (16), 117 (15), 106 (8), 89 (9), 75 (9), 63 (29). Anal. Calcd for $C_{11}H_{12}O_3$: C, 68.74; H, 6.29. Found: C, 68.60; H, 6.23.

4.1.9.2. 6-Ethynyl-4-methoxy-1,3-benzodioxole (11b).[71] White solid, yield 91%, mp 63–64 °C. ^{1}H NMR ($CDCl_3$): δ 2.96 (s, 1H, CH), 3.88 (s, 3H, OCH_3), 5.98 (s, 2H, OCH_2O), 6.66 (d, J = 1.4 Hz, 1H, H-5), 6.70 (d, J = 1.4 Hz, 1H, H-7). EIMS *m/z* 176 $[M]^+$ (100), 161 (7), 131 (30), 103 (13), 75 (44), 63 (13). Anal. Calcd for $C_{10}H_8O_3$: C, 68.18; H, 4.58. Found: C, 68.32; H, 4.65.

4.1.9.3. 5-Ethynyl-4,7-dimethoxy-1,3-benzodioxole (11c). White solid, yield 90%, mp 54–56 °C. ^{1}H NMR ($CDCl_3$): δ 3.20 (s, 1H, CH), 3.85 (s, 3H, OCH_3-4), 4.00 (s, 3H, OCH_3-7), 6.00 (s, 2H, OCH_2O), 6.64 (s, 1H, H-5). EIMS *m/z* 206 $[M]^+$ (100), 191 (60), 161 (13), 135 (13), 133 (22), 118 (10), 107 (23), 105 (27), 103 (11), 101 (15), 92 (38), 90 (26), 83 (23), 77 (67). Anal. Calcd for $C_{11}H_{10}O_4$: C, 64.07; H, 4.89. Found: C, 63.94; H, 4.81.

4.1.10. General procedure for the synthesis of 1,2-diarylalkynes (12)

Diethylamine (14.5 mL) was added with syringe to the mixture of $(PPh_3)_4Pd$ (0.168 g, 0.146 mmol), CuI (0.055 g, 0.291 mmol), 4-iodoanizole (3.41 g, 14.57 mmol), and arylalkyne (14.57 mmol) under Ar. The solution was stirred at 50 °C for 2 h and overnight at rt, then diethylamine was evaporated, and the residue was diluted with water. Diarylalkynes **12ad'** and **12bd'** as crude solid deposits were filtered off, washed with water, and dried *in vacuo*, yielding pale yellow products. Oily **12cd'** was extracted from the mixture with ethyl acetate, dried over $MgSO_4$, the solvent was removed under reduced pressure, and the residue was dried *in vacuo*, yielding pale yellow diarylalkyne. **12ad'**, **12bd'**, and **12cd'** were purified by flash chromatography on silica gel (toluene–heptane–ethylacetate = 1:1:0.4) and crystallized from methanol to afford colorless crystals.

4.1.10.1. 1,2,3-Trimethoxy-5-(4-methoxyphenylethynyl)benzene (12ad'). Colorless solid, yield 97%, mp 114–115 °C (lit.[72] 119–121 °C). ^{1}H NMR ($CDCl_3$): δ 3.83 (s, 3H, OCH_3-4), 3.87 (s, 3H, OCH_3-4'),

3.88 (s, 6H, 2 x OCH_3-3,5), 6.76 (s, 2H, H-2,6), 6.88 (d, *J* = 8.8 Hz, 2H, H-3',5'), 7.47 (d, *J* = 8.8 Hz, 2H, H-2',6'). EIMS *m/z* 298 $[M]^+$ (100), 283 (77), 268 (2), 255 (16), 240 (8), 225 (16), 223 (11), 212 (12), 195 (9), 169 (21), 149 (27), 134 (18), 126 (19), 119 (15), 113 (14), 91 (8), 85 (19), 69 (29), 63 (10). Anal. Calcd for $C_{18}H_{18}O_4$: C, 72.47; H, 6.08. Found: C, 72.34; H, 6.00.

4.1.10.2. 4-Methoxy-6-[(4-methoxyphenyl)ethynyl]-1,3-benzodioxole (12bd'). Colorless solid, yield 88%, mp 88–90 °C. ^{1}H NMR ($CDCl_3$): δ 3.83 (s, 3H, OCH_3-4'), 3.92 (s, 3H, OCH_3-4), 5.99 (s, 2H, OCH_2O), 6.69 (d, *J* = 1.4 Hz, 1H, H-5), 6.73 (d, *J* = 1.4 Hz, 1H, H-7), 6.87 (d, *J* = 8.9 Hz, 2H, H-3',5'), 7.44 (d, *J* = 8.9 Hz, 2H, H-2',6'). EIMS *m/z* 282 $[M]^+$ (100), 267 (38), 239 (14), 237 (10), 181 (9), 166 (18), 152 (15), 150 (16), 141 (36), 138 (33), 113 (18), 91 (19), 87 (17), 86 (17), 75 (15), 63 (16). Anal. Calcd for $C_{17}H_{14}O_4$: C, 72.33; H, 5.00. Found: C, 72.49; H, 5.07.

4.1.10.3. 4,7-Dimethoxy-5-[(4-methoxyphenyl)ethynyl]-1,3-benzodioxole (12cd'). Colorless solid, yield 92%, mp 58–60 °C. ^{1}H NMR ($CDCl_3$): δ 3.82 (s, 3H, OCH_3-4'), 3.86 (s, 3H, OCH_3-7), 4.03 (s, 3H, OCH_3-4), 6.00 (s, 2H, OCH_2O), 6.66 (s, 1H, H-6), 6.86 (d, *J* = 8.8 Hz, 2H, H-3',5'), 7.46 (d, *J* = 8.8 Hz, 2H, H-2',6'). EIMS *m/z* 312 $[M]^+$ (100), 297 (23), 282 (3), 267 (4), 239 (7), 198 (16), 183 (9), 171 (10), 156 (31), 151 (11), 147 (7), 113 (6), 82 (13), 63 (13). Anal. Calcd for $C_{18}H_{16}O_5$: C, 69.22; H, 5.16. Found: C, 69.09; H, 5.10.

4.1.11. General procedure for the synthesis of isomer mixture of 1-benzyl-4(5),5(4)-diaryl-1,2,3-triazoles (13)

For the procedure a barostat with the capacity of 40 tons and operating temperatures up to 200 °C was used.[73] A solution of 1,2-diarylalkyne (2 mmol) and benzylazide (0.346 g, 2.60 mmol) in DMF (1 mL) was poured into a Teflon vial and inserted into barostat thick-walled steel cylinder. The reaction mixture was heated at 100 °C for 7 h under 15 kbar, and then was cooled to rt overnight. Solvent was evaporated *in vacuo* (20 °C, 0.1 mbar). The residue was purified by column chromatography on silica gel (eluent toluene–heptane–ethylacetate = 2:1:1) to yield a mixture of isomers in ratio ~1:1 to 1:1.5 as a colorless viscous oil, which was used for the next hydrogenation step.

4.1.11.1. Mixture of 1-benzyl-4-(4-methoxyphenyl)-5-(-(3,4,5-trimethoxyphenyl)-1*H*-1,2,3-triazole (13a'd) and 1-benzyl-5-(4-methoxyphenyl)-4-(3,4,5-trimethoxyphenyl)-1*H*-1,2,3-triazole (13ad').

Colorless viscous oil, yield 88%. Ratio of isomers: **13ad'** : **13a'd** = 1 : 1.3. In a representative experiment, the reaction mixture (1-benzyl-4(5)-(4-methoxyphenyl)-5(4)-(3,4,5-trimethoxyphenyl)-1*H*-1,2,3-triazole) was separated using column chromatography to yield a single isomer. Its structure was determined unequivocally using NOESY experiment. Specifically, we observed an inter-space interaction of the *N*CH_2 with protons H-2''',6''' allowing to assign the structure **13a'd**. The ^{1}H NMR signals of isomers in other mixtures were assigned in a similar way.

4.1.11.2. 1-Benzyl-5-(4-methoxyphenyl)-4-(3,4,5-trimethoxyphenyl)-1*H*-1,2,3-triazole (13ad').

Colorless viscous oil, yield 38%. ^{1}H NMR ($CDCl_3$): δ 3.65 (s, 6H, 2 × OCH_3-3'',5''), 3.81 (s, 3H, OCH_3-4'''), 3.85 (s, 3H, OCH_3-4''), 5.40 (s, 2H, NCH_2), 6.84 (s, 2H, H-2'',6''), 6.95 (d, *J* = 8.7 Hz, 2H, H-3''',5'''), 7.06 (d, *J* = 7.5 Hz, 2H, H-2',6'), 7.08 (d, *J* = 8.7 Hz, 2H, H-2''',6'''), 7.28 (m, 3H, H-3',4',5').

4.1.11.3. 1-Benzyl-4-(4-methoxyphenyl)-5-(3,4,5-trimethoxyphenyl)-1*H*-1,2,3-triazole (13a'd).

White solid, yield 50%, mp 136–138 °C. ^{1}H NMR ($CDCl_3$): δ 3.61 (s, 6H, 2 × OCH_3-3''',5'''), 3.79 (s, 3H, OCH_3-4''), 3.92 (s, 3H, OCH_3-4'''), 5.41 (s, 2H, NCH_2), 6.26 (s, 2H, H-2''',6'''), 6.83 (d, *J* = 8.7 Hz, 2H, H-3'',5''), 7.07 (d, *J* = 7.5 Hz, 2H, H-2',6'), 7.28 (m, 3H, H-3',4',5'), 7.56 (d, *J* = 8.7 Hz, 2H, H-2'',6''). NMR ^{13}C ($CDCl_3$, 125.76 MHz): δ 52.12 (OCH_3-4'''), 55.22 (OCH_3-4''), 56.02 (2 × OCH_3-3''',5'''), 61.01 (CH_2N), 107.09 (C-2''',6'''), 113,89 (C-3'',5''), 123.01 (C-1''), 123.50 (C-1'''), 127.28 (C-2',6'), 127.80 (C-3',5'), 128.07 (C-4'), 128.73 (C-2'',6''), 132.93 (C-4), 136.02 (C-1'), 138.76 (C-5), 144.16 (C-4'''), 153.61 (C-3''',5'''), 159.23 (C-4''). EIMS *m/z* 431 $[M]^+$ (17), 340 (1), 313 (20), 312 (100), 296 (2), 282 (4), 266 (5), 251 (4), 178 (4), 140 (7), 119 (6), 91 (70), 65 (21). Anal. Calcd for $C_{25}H_{25}N_3O_4$: C, 69.59; H, 5.84; N, 9.74. Found: C, 69.76; H, 5.91; N, 9.58.

4.1.11.4. Mixture of 1-benzyl-5-(4-methoxyphenyl)-4-(7-methoxy-1,3-benzodioxol-5-yl)-1*H*-1,2,3-triazole (13bd') and 1-benzyl-4-(4-methoxyphenyl)-5-(7-methoxy-1,3-benzodioxol-5-yl)-1*H*-1,2,3-

triazole (13b'd). Colorless viscous oil, yield 84%. Ratio of isomers in a mixture: **13bd'** : **13b'd** = 1 : 1.2.

4.1.11.5. 1-Benzyl-5-(4-methoxyphenyl)-4-(7-methoxy-1,3-benzodioxol-5-yl)-1*H*-1,2,3-triazole (13bd'). Colorless viscous oil, yield 38%. ^{1}H NMR ($CDCl_3$): δ 3.76 (s, 3H, OCH_3-7''), 3.86 (s, 3H, OCH_3-4'''), 5.37 (s, 2H, NCH_2), 5.92 (s, 2H, OCH_2O), 6.63 (s, 1H, H-6''), 6.94 (d, J = 8.7 Hz, 2H, H-3''',5'''), 6.95 (s, 1H, H-4''), 7.04 (d, J = 7.6 Hz, 2H, H-2',6'), 7.05 (d, J = 8.7 Hz, 2H, H-2''',6'''), 7.27 (m, 3H, H-3',4',5').

4.1.11.6. 1-Benzyl-4-(4-methoxyphenyl)-5-(7-methoxy-1,3-benzodioxol-5-yl)-1*H*-1,2,3-triazole (13b'd). Colorless viscous oil, yield 46%. ^{1}H NMR ($CDCl_3$): δ 3.62 (s, 3H, OCH_3-7'''), 3.79 (s, 3H, OCH_3-4''), 5.40 (s, 2H, NCH_2), 6.06 (s, 2H, OCH_2O), 6.15 (s, 1H, H-6'''), 6.33 (s, 1H, H-4'''), 6.83 (d, J = 8.7 Hz, 2H, H-3'',5''), 7.08 (d, J = 7.6 Hz, 2H, H-2',6'), 7.27 (m, 3H, H-3',4',5'), 7.54 (d, J = 8.7 Hz, 2H, H-2'',6'').

4.1.11.7. Mixture of 1-Benzyl-5-(4-methoxyphenyl)-4-(4,7-dimethoxy-1,3-benzodioxol-5-yl)-1*H*-1,2,3-triazole (13cd') and 1-Benzyl-4-(4-methoxyphenyl)-5-(4,7-dimethoxy-1,3-benzodioxol-5-yl)-1*H*-1,2,3-triazole (13c'd). Colorless viscous oil, yield 98%. Ratio of isomers: **13cd'** : **13c'd** = 1 : 1.07.

4.1.11.8. 1-Benzyl-5-(4-methoxyphenyl)-4-(4,7-dimethoxy-1,3-benzodioxol-5-yl)-1*H*-1,2,3-triazole (13cd'). Colorless viscous oil, yield 47%. ^{1}H NMR ($CDCl_3$): δ 3.38 (s, 3H, OCH_3-4''), 3.57 (s, 3H, OCH_3-7''), 3.81 (s, 3H, OCH_3-4'''), 5.19 and 5.57 (two d, J = 12.1 Hz, 2H, NCH_2), 5.97 (s, 2H, OCH_2O), 6.69 (s, 1H, H-6''), 6.87 (d, J = 8.5 Hz, 2H, H-3''',5'''), 7.03 (d, J = 8.5 Hz, 2H, H-2''',6'''), 7.04 (d, J = 7.5 Hz, 2H, H-2',6'), 7.23 (m, 3H, H-3',4',5').

4.1.11.9. 1-Benzyl-4-(4-methoxyphenyl)-5-(4,7-dimethoxy-1,3-benzodioxol-5-yl)-1*H*-1,2,3-triazole (13c'd). Colorless viscous oil, yield 51%. ^{1}H NMR ($CDCl_3$): δ 3.57 (s, 3H, OCH_3-7'''), 3.78 (s, 3H, OCH_3-4''), 3.82 (s, 3H, OCH_3-4'''), 5.48 (s, 2H, NCH_2), 5.97 (s, 1H, H-6'''), 6.08 (s, 2H, OCH_2O), 6.83 (d, J = 8.7 Hz, 2H, H-3'',5''), 7.11 (d, J = 7.6 Hz, 2H, H-2',6'), 7.29 (m, 3H, H-3',4',5'), 7.56 (d, J = 8.7 Hz, 2H, H-2'',6'').

4.1.12. General procedure for the synthesis of 1*H*-4,5-diaryl-1,2,3-triazoles (14)

A solution of isomers 1-benzyl-4(5),5(4)-diaryl-1,2,3-triazole (**13**) (1,5 mmol) in a mixture of methanol (25 mL) and trifluoroacetic acid (2 mL) was hydrogenated over 10% Pd/C catalyst (400 mg) at 55 °C under 20 bar for 50 h. The resulting mixture was filtered through celite, and solvent was removed *in vacuo*. The residue was dissolved in ethylacetate, washed with saturated solution of $NaHCO_3$ and brine, and then dried over $MgSO_4$. After solvent evaporation the resulting pellet was purified by column chromatography on silica gel (eluent toluene–ethylacetate = 2:1) to yield targeted triazole as colorless solid.

4.1.12.1. 4-(4-Methoxyphenyl)-5-(3,4,5-trimethoxyphenyl)-1*H*-1,2,3-triazole (14ad'). Colorless solid, yield 91%, mp 173–175 °C. ^{1}H NMR ($CDCl_3$): δ3.73 (s, 6H, OCH_3-3",5"), 3.82 (s, 3H, OCH_3-4"), 3.88 (s, 3H, OCH_3-4'), 6.83 (s, 2H, H-2",6"), 6.91 (d, J = 8.8 Hz, 2H, H-3',5'), 7.51 (d, J = 8.8 Hz, 2H, H-2',6'), 11.50 (s, 1H, NH). EIMS *m/z* 341 $[M]^+$ (100), 326 (45), 313 (3), 298 (4), 266 (10), 251 (15), 223 (11), 212 (9), 169 (15), 153 (10), 140 (15), 133 (17), 127 (10), 120 (13), 119 (12), 114 (15), 105 (12), 93 (11), 90 (17), 77 (24), 76 (32). Anal. Calcd for $C_{18}H_{19}N_3O_4$: C, 63.33; H, 5.61; N, 12.31. Found: C, 63.46; H, 5.67; N, 12.17.

4.1.12.2. 4-(4-Methoxyphenyl)-5-(7-methoxy-1,3-benzodioxol-5-yl)-1*H*-1,2,3-triazole (14bd'). Colorless solid, yield 95%, mp 78–80 °C. ^{1}H NMR ($CDCl_3$): δ3.81 (s, 3H, OCH_3-7'), 3.84 (s, 3H, OCH_3-4"), 6.00 (s, 2H, OCH_2O), 6.72 (d, J = 1.3 Hz, 1H, H-6'), 6.78 (d, J = 1.3 Hz, 1H, H-4'), 6.93 (d, J = 8.8 Hz, 2H, H-3",5"), 7.50 (d, J = 8.8 Hz, 2H, H-2",6"), 12.15 (s, 1H, NH). EIMS *m/z* 325 $[M]^+$ (100), 297 (5), 255 (6), 197 (7), 181 (6), 169 (10), 153 (12), 147 (7), 140 (6), 131 (10), 126 (15), 119 (5), 90 (8), 77 (11), 76 (16). Anal. Calcd for $C_{17}H_{15}N_3O_4$: C, 62.76; H, 4.65; N, 12.92. Found: C, 62.84; H, 4.68; N, 12.86.

4.1.12.3. 4-(4-Methoxyphenyl)-5-(4,7-dimethoxy-1,3-benzodioxol-5-yl)-1*H*-1,2,3-triazole (14cd'). Colorless solid, yield 90%, mp 135–137 °C. ^{1}H NMR (DMSO-d_6): δ3.46 (s, 3H, OCH_3-4'), 3.75 (s, 3H, OCH_3-7'), 3.76 (s, 3H, OCH_3-4"), 6.09 (s, 2H, OCH_2O), 6.59 (s, 1H, H-6'), 6.95 (d, J = 8.8 Hz, 2H, H-

3",5"), 7.40 (d, J = 8.8 Hz, 2H, H-2",6"), 14.90 (s, 1H, NH). EIMS *m/z* 355 $[M]^+$ (100), 327 (3), 326 (3), 312 (9), 310 (3), 282 (8), 156 (6), 133 (5), 92 (7), 91 (15), 77 (9), 69 (10). Anal. Calcd for $C_{18}H_{17}N_3O_5$: C, 60.84; H, 4.82; N, 11.83. Found: C, 60.89; H, 4.85; N, 11.81.

4. 2. Sea urchin embryo assay[44]

Adult sea urchins, *Paracentrotus lividus* L. (Echinidae), were collected from the Mediterranean Sea on the Cyprus coast and kept in an aerated seawater tank. Gametes were obtained by intracoelomic injection of 0.5 M KCl. Eggs were washed with filtered seawater and fertilized by adding drops of diluted sperm. Embryos were cultured at room temperature under gentle agitation with a motor-driven plastic paddle (60 rpm) in filtered seawater. The embryos were observed with a Biolam light microscope (LOMO, St. Petersburg, Russia). For treatment with the test compounds, 5 mL aliquots of embryo suspension were transferred to six-well plates and incubated as a monolayer at a concentration up to 2000 embryos/mL. Stock solutions of compounds were prepared in DMSO at 10 mM concentration followed by a 10-fold dilution with 95% EtOH. This procedure enhanced the solubility of the test compounds in the salt-containing medium (seawater), as evidenced by microscopic examination of the samples. The maximal tolerated concentrations of DMSO and EtOH in the in vivo assay were determined to be 0.05% and 1%, respectively. Higher concentrations of either DMSO (≥0.1%) or EtOH (>1%) caused nonspecific alteration and retardation of the sea urchin embryo development independent of the treatment stage. Combretastatins A-4 and A-2 (synthesized according to ref [50]) served as reference compounds. The antiproliferative activity was assessed by exposing fertilized eggs (8–20 min after fertilization, 45–55 min before the first mitotic cycle completion) to 2-fold decreasing concentrations of the compound. Cleavage alteration and arrest were clearly detected at 2.5–5.5 h after fertilization. The effects were estimated quantitatively as an effective threshold concentration, resulting in cleavage alteration and embryo death before hatching or full mitotic arrest. At these concentrations all tested microtubule destabilizers caused 100% cleavage alteration and embryo death before hatching, whereas at 2-fold lower concentrations the compounds failed to produce any effect. For microtubule-

destabilizing activity, the compounds were tested on free-swimming blastulae just after hatching (8–10 h after fertilization), which originated from the same embryo culture. Embryo spinning was observed after 15 min to 20 h of treatment, depending on the structure and concentration of the compound. Both spinning and lack of forward movement were interpreted to be the result of the microtubule-destabilizing activity of a molecule. Video illustrations are available at http://www.chemblock.com. Both sea urchin embryo assay and DTP NCI60 cell line activity data are available free of charge via the Internet at http://www.zelinsky.ru.

4. 3. Jurkat and Jurkat A4 cell-based assays

4.3.1. Cell culture and morphology

Human T-cell acute lymphoblastic leukemia line Jurkat was obtained from the National Collection of Cell Lines of Institute of Experimental Pathology, Oncology and Radiobiology (Kyiv, Ukraine). The CD95-deficient cell clone Jurkat/A4 was derived from the Jurkat cell line by serial treatment with apoptosis-inducing anti-CD95 MAb (clone IPO-4, class IgM).[45] The cells were maintained at 37 °C in an atmosphere of 95% air and 5% CO_2 as suspension cultures in RPMI-1640 medium supplemented with 10% fetal calf serum. The cultures were passaged every 3–4 days immediately upon reaching maximum cell density. For studying cell morphology, cells were cytospined and stained by May–Grünwald–Giemsa (MGG) technique. Light microscopy images (100× objective) were recorded by Axiostar 2 plus Axio Cam MRc5 (Zeiss).

4.3.2. Cytotoxicity assay

CA4 disodium phosphate (CA4P, obtained from OxiGene, USA), served as a reference compound in all cell-based assays. **10ad'** and CA4P were added at exponential growth phase. Cell viability was assessed in 96-well microplates by direct counting of trypan blue dye-excluding cells. EC_{50} values were determined by linear interpolation of cell survival data after 48 h of treatment.

4.3.3. Cell cycle analysis and apoptosis estimation

Cell cycle analysis and apoptosis in Jurkat and Jurkat A4 cells were assessed by flow cytometry. The cells were resuspended in hypotonic lysis buffer containing 0.1% sodium citrate, 0.1% Triton X-100, 5 μg/ml propidium iodide (PI). 250 μg/ml of RNAse A was added to each sample, and the cells were stained for 15 min at 37 °C. Flow cytometry was performed on a BD™ FACSCalibur system (Becton Dickinson, USA). Forward and sideways light scattering provided the elimination of dead cells and debris. The fluorescence of PI-stained cells was measured by flow cytometry. Data were analyzed using ModFit LT 2.0 (Verity Software House, Topsham, ME), or CellQuest software package (BD Biosciences).

For the study of caspase involvement in the compound-induced cell death, cells were pre-incubated with a pancaspase inhibitor z-VAD-fmk[74] at concentration of 50 μM for 3 h. Then cells were exposed to **10ad'** or CA4P for 48 h at concentrations 30 and 15 nM for Jurkat cells, or 300 and 150 nM for Jurkat/A4 cells, respectively.

4.3.4. SDS-PAGE and Western blotting

After incubation with **10ad'** or CA4P for 24 or 48 h, cells were collected, centrifuged, and washed twice with ice cold PBS. The pellet was resuspended in lysis buffer containing 20 mM Tris-HCl (pH 7.4), 1% Triton X-100, and 150 mM NaCl, with freshly added protease inhibitor cocktail (Roche, Germany) for 30 min at 4 °C. The lysates were centrifuged at 15,000 rpm at 4 °C for 10 min. Protein concentration was estimated according to published procedure.[75] Equal amounts of protein were resolved using sodium dodecyl sulfate–polyacrylamide gel electrophoresis (SDS–PAGE) (12% acrylamide gels) and transferred to PVDF membrane (Immobilon-P, Millipore, USA). Membranes were blocked with 5% skim milk in PBS containing 0.05% Tween 20 followed by incubation with primary monoclonal antibodies (MoAb) against caspase-9 (clone 2-22), caspase-8 (clone 3-1-9), caspase-2 (clone 35/Caspase-2/ICH-1L), Bcl-2 (B-cell lymphoma 2, clone 7/Bcl-2), or XIAP (X-linked inhibitor of apoptosis, clone 28/hILP/XIAP) (all purchased from BD Biosciences) for 2 h at room temperature.

Then HRP-conjugated goat anti-mouse antibodies (Promega, USA) were added to membranes for 60 min. Membranes were visualized using ECL detection system (Amersham Pharmacia, UK). To confirm equal protein loading, each membrane was probed with anti-β-actin MoAb (clone AC-15, Sigma, USA). Anti-caspase 8 (clone 5F7 recognizing the proform of caspase-8) and anti-caspase 9 (clone 5B4) monoclonal antibodies (MAbs) were obtained from Immunotech (France). Anti-caspase 2 MAb (clone 35) was obtained from BD Pharmingen Transduction Laboratories (USA).

4.3.5. Caspase-3 activation and PARP-1 cleavage

The percentage of cells containing active form of caspase-3 or cleaved form of PARP-1 (poly(ADP-ribose) polymerase-1) was assessed by flow cytometry using Caspase-3, Active Form, mAb Apoptosis Kit: FITC (BD Biosciences) or FITC-conjugated MoAb (clone F21-852; BD Biosciences), correspondingly. Prior to immunostaining, the cells were permeabilized according to the procedure recommended by the manufacturer.

4.3.6. Statistical analysis

The Student's *t*-test was used as appropriate. Statistical significance was accepted at a P value of < 0.05.

Acknowledgments

This work was supported by the grant # 13-03-90455 from Russian Foundation for Basic Research *(*RFBR), grant # F53.4/056 from State Fund for Fundamental Research (DFFD), Ukraine, and a grant from Chemical Block Ltd. We thank the National Cancer Institute (NCI) (Bethesda, MD, USA) for screening compounds **5aa'**, **5dd'**, **5fa'**, **5fe'**, **6aa'**, **6ad'**, **7da'**, **8ad'**, **8da'**, **9da'**, **10bd'**, **14ad'**, **14bd'**, and **14cd'** by the Developmental Therapeutics Program at NCI (Anticancer Screening Program; http://dtp.cancer.gov).

References and notes

1. Pettit, G. R.; Singh, S. B.; Niven, M. L.; Hamel, E.; Schmidt, J. M. *J. Nat. Prod.* **1987**, *50*, 119.
2. Pettit, G. R.; Singh, S. B. *Can. J. Chem.* **1987**, *65*, 2390.

3. Pettit, G. R.; Singh, S. B.; Hamel, E.; Lin, C. M.; Alberts, D. S.; Garcia-Kendall, D. *Experientia* **1989**, *45*, 209.
4. Lin, C. M.; Singh, S. B.; CHu, S. P.; Dempcy, R. O.; Schmidt, J. M.; Pettit, G. R.; Hamel, E. *Mol. Pharmacol.* **1988**, *34*, 200.
5. Lin, C. M.; Ho, H. H.; Pettit, G. R.; Hamel, E. *Biochemistry* **1989**, *28*, 6984.
6. Pettit, G. R.; Temple, C. Jr.; Narayanan, V. L.; Varma, R.; Simpson, M. J.; Boyed, M. R.; Rener, G. A.; Bansal, N. *Anti-Cancer Drug Des.* **1995**, *10*, 299.
7. Kingston, D. G. I. *J. Nat. Prod* **2009**, *72*, 507.
8. Siemann, D. W.; Chaplin, D. J.; Walicke, P. A. *Expert Opin. Invest. Drugs* **2009**, *18*, 189.
9. Siemann, D. W. *Cancer Treat. Rev.* **2011**, *37*, 63.
10. Cooney, M. M.; Radivoyevitch, T.; Dowlati, A.; Overmoyer, B.; Levitan, N.; Robertson, K.; Levine, S. L.; DeCaro, K.; Buchter, C.; Taylor, A.; Stambler, B. S.; Remick, S. C. *Clin. Cancer Res.* **2004**, *10*, 96.
11. Bhakta, S.; Flick, S. M.; Cooney, M. M.; Greskovich, J. F.; Gilkeson, R. C.; Remick, S. C.; Ortiz, J. *Clin. Cardiol.* **2009**, *32*, E80.
12. http://www.cancertreatment.org.uk/research/blood-tumor.html
13. Nam, N.-H. *Curr. Med. Chem.* **2003**, *10*, 1697.
14. Tron, G. C.; Pyrali, T.; Sorba, G.; Pagliai, F.; Busacca, S.; Genazzani, A. A. *J. Med. Chem.* **2006**, *49*, 3033.
15. Cushman, M.; Nagarathnam, D.; Gopal, D.; Chakraborti, A. K.; Lin, C. M.; Hamel, E. *J. Med. Chem.* **1991**, *34*, 2579.
16. Aprile, S.; Del Grosso, E.; Tron, G. C.; Grosa, G. *Drug Metab. Dispos.* **2007**, *35*, 2252.
17. Biersack, B.; Effenberger, K.; Knauer, S.; Ocker, M.; Schobert, R. *Eur. J. Med. Chem.* **2010**, *45*, 4890.

18. Kaffy, J.; Pontikis, R.; Carrez, D.; Croisy, A.; Monneret, C.; Florent, J. C. *Bioorg. Med. Chem.* **2006**, *14*, 4067.

19. Sun, C. M.; Lin, L. G.; Yu, H. J.; Cheng, C. Y.; Tsai, Y. C.; Chu, C. W.; Din, Y. H.; Chau, Y. P.; Don, M. J. *Bioorg. Med. Chem. Lett.* **2007**, *17*, 1078.

20. Romagnoli, R.; Baraldi, P. G.; Brancale, A.; Ricci, A.; Hamel, E.; Bortolozzi, R.; Basso, G.; Viola, G. *J. Med. Chem.* **2011**, *54*, 5144.

21. Liu, T.; Dong, X.; Xue, N.; Wu, R.; He, Q.; Yang, B.; Hua, Y. *Bioorg. Med. Chem.* **2009**, *17*, 6279.

22. Xue, N.; Yang, X.; Wu, R.; Chen, J.; He, Q.; Yang, B.; Lu, X.; Hu, Y. *Bioorg. Med. Chem.* **2008**, *16*, 2550.

23. Burja, B.; Cimbora-Zovko, T.; Tomic, S.; Jelusic, T.; Kocevar, M.; Polanc, S.; Osmak, M. *Bioorg. Med. Chem.* **2010**, *18*, 2375.

24. Liu, T.; Cui, R.; Chen, J.; Zhang, J.; He, Q.; Yang, B.; Hu, Y. *Arch. Pharm. Chem. Life Sci.* **2011**, *11*, 279.

25. Tsyganov, D. V.; Konyushkin, L. D.; Karmanova, I. B.; Firgang, S. I.; Strelenko, Y. A.; Semenova, M. N.; Kiselyov, A. S.; Semenov, V. V. *J. Nat. Prod.* **2013**, *76*, 1485.

26. Romagnoli, R.; Baraldi, P. G.; Salvador, M. K.; Preti, D.; Aghazadeh, T. M.; Brancale, A.; Fu, X. H.; Li, J.; Zhang, S. Z.; Hamel, E.; Bortolozzi, R.; Basso, G.; Viola, G. *J. Med. Chem.* **2011**, *55*, 475.

27. Zhang, Q.; Peng, Y.; Wang, X. I.; Keenan, S. M.; Arora, S.; Welsh, W. J. *J. Med. Chem.* **2007**, *50*, 749.

28. Romagnoli, R.; Baraldi, P. G.; Cruz-Lopez, O.; Lopez Cara, C.; Carrion, M. D.; Brancale, A.; Hamel, E.; Chen, L.; Bortolozzi, R.; Basso, G.; Viola, G. *J. Med. Chem.* **2010**, *53*, 4248.

29. Pati, H. N.; Wicks, M.; Holt, H. L. Jr.; LeBlanc, R.; Weisbruch, P.; Forrest, L.; Lee, M. *Heterocycl. Commun* **2005**, *11*, 117.

30. Cafici, L.; Pirali, T.; Condorelli, F.; Del Grosso, E.; Massarotti, A.; Sorba, G.; Canonico, P. L.; Tron, G. C.; Genazzani, A. A. *J. Comb. Chem.* **2008**, *10*, 732.

31. Odlo, K.; Hentzen, J.; dit Chabert, J. F.; Ducki, S.; Gani, O. A. B. S.; Sylte, I.; Skrede, M.; Florenes, V. A.; Hansen, T. V. *Biorg. Med. Chem.* **2008**, *16*, 4829.

32. Odlo, K.; Fournier-Dit-Chabert, J.; Ducki, S.; Gani, O. A. B. S.; Sylte, I.; Hansen, T. V. *Bioorg. Med. Chem.* **2010**, *18*, 6874.

33. Akselsen, Q. W.; Odlo, K.; Cheng, J. J.; Maccari, G.; Botta, M.; Hansen, T. V. *Bioorg. Med. Chem.* **2012**, *20*, 234.

34. Beale, T. M.; Bond, P. J.; Brenton, J. D.; Charnock-Jones, D. S.; Ley, S. V.; Myers, R. M. *Biorg. Med. Chem.* **2012**, *20*, 1749.

35. Aziz, G.; Odlo, K.; Hansen, T. V.; Paulsen, R. E.; Mathisen, G. H. *Eur. J. Med. Chem.* **2013**, *703*, 25.

36. Romagnoli, R.; Baraldi, P. G.; Salvador, M. K.; Preti, D.; Tabrizi, M. A.; Brancale, A.; Fu, X.-H.; Li, J.; Zhang, S.-Z.; Hamel, E.; Bortolozzi, R.; Basso, G.; Viola, G. *J. Med. Chem.* **2012**, *55*, 475.

37. Ohsumi, K.; Hatanaka, T.; Fujita, K.; Nakagawa, R.; Fukuda, Y.; Nihei, Y.; Suga, Y.; Morinaga, Y.; Akiyama, Y.; Tsuji, T. *Bioorg. Med. Chem. Lett.* **1998**, *8*, 3153.

38. Tsyganov, D. V.; Khrustalev, V. N.; Konyushkin, L. D.; Raihstat, M. M.; Firgang, S. I.; Semenov, R. V.; Kiselyov, A. S.; Semenova, M. N.; Semenov, V. V. *Eur. J. Med. Chem.* **2013**, *in press.*

39. Demko, Z.; Borella, C.; Chen, S.; Sun, L. **US Patent 2007238699 A1**, 2007.

40. Billard, C.; Menasria, F.; Quiney, C.; Faussat, A.-M.; Finet, J.-P.; Combes, S.; Kolb, J.-P. *Exp. Hematol.* **2008**, *36*, 1625.

41. Horsman, M. R.; Ehrnrooth, E.; Ladekarl, M.; Overgaard, J. *Int. J. Radiat. Oncol.* **1998**, *42*, 895.

42. Greene, L. M.; O'Boyle, N. M.; Nolan, D. P.; Meegan, M. J.; Zisterer, D. M. *Biochem. Pharmacol.* **2012**, *84*, 612.

43. Cenciarelli, C.; Tanzarella, C.; Vitale, I.; Pisano, C.; Crateri, P.; Meschini, S.; Arancia, G.; Antoccia, A. *Apoptosis* **2008**, *13*, 659.

44. Semenova, M. N.; Kiselyov, A. S.; Semenov, V. V. *BioTechniques* **2006**, *40*, 765.

45. Sokolovskaia, A. A.; Zabotina, T. N.; Blokhin, D. Yu.; Inshakov, A. N.; Mikhailov, A. D.; Kadagidze, Z. G.; Baryshnikov, A. Y. *Exp. Oncol.* **2001**, *23*, 175.

46. Semenova, M. N.; Kiselyov, A. S.; Titov, I. Y.; Molodtsov, M.; Grishchuck, E.; Spiridonov, I.; Semenov, V. V. *Chem. Biol. Drug. Des.* **2007**, *70*, 485.

47. Kiselyov, A. S.; Semenova, M. N.; Chernyshova, N. B.; Leitao, A.; Samet, A. V.; Kislyi, K. A.; Raihstat, M. M.; Oprea, T.; Lemcke, H.; Lantow, M.; Weiss, D. G.; Ikizalp, N. N.; Kuznetsov, S. A.; Semenov, V. V. *Eur. J. Med. Chem.* **2010**, *45*, 1683.

48. Semenova, M. N.; Kiselyov, A. S.; Tsyganov, D. V.; Konyushkin, L. D.; Firgang, S. I.; Semenov, R. V.; Malyshev, O. R.; Raihstat, M. M.; Fuchs, F.; Stielow, A.; Lantow, M.; Philchenkov, A. A.; Zavelevich, M. P.; Zefirov, N. S.; Kuznetsov, S. A.; Semenov, V. V. *J. Med. Chem.* **2011**, *54*, 7138.

49. Semenov, V. V.; Rusak, V. A.; Chartov, E. M.; Zaretsky, M. I.; Konyushkin, L. D.; Firgang, S. I.; Chizhov, A. O.; Elkin, V. V.; Latin, N. N.; Bonashek, V. M.; Stas'eva, O. N. *Russ. Chem. Bull.* **2007**, *56*, 2448.

50. Semenov, V. V.; Kiselyov, A. S.; Titov, I. Y.; Sagamanova, I. K.; Ikizalp, N. N.; Chernysheva, N. B.; Tsyganov, D. V.; Konyushkin, L. D.; Firgang, S. I.; Semenov, R. V.; Karmanova, I. B.; Raihstat, M. M.; Semenova, M. N. *J. Nat. Prod.* **2010**, *73*, 1796.

51. Hu, M.; Li, J.; Yao, S. Q. *Org. Lett.* **2008**, *10*, 5529.

52. Danence, L. J. T.; Gao, Y.; Li, M.; Huang, Y.; Wang, J. *Chem. Eur. J.* **2011**, *17*, 3584.

53. Pettit, G. R.; Singh, S. B.; Boyd, M. R.; Hamel, E.; Pettit, R. K.; Schmidt, J. M.; Hogan, F. *J. Med. Chem.* **1995**, *38*, 1666.

54. Pettit, G. R.; Anderson, C. R.; Herald, D. L.; Jung, M. K.; Lee, D. J.; Hamel, E.; Pettit, R. K. *J. Med. Chem.* **2003**, *46*, 525.

55. O'Boyle, N. M.; Carr, M.; Greene, L. M.; Keely, N. O.; Knox, A. J.; McCabe, T.; Lloyd, D. G.; Zisterer, D. M.; Meegan, M. J. *Eur. J. Med. Chem.* **2011**, *46*, 4595.

56. Galluzzi, L.; Vitale, I.; Abrams, J. M.; Alnemri, E. S.; Baehrecke, E. H.; Blagosklonny, M. V.; Dawson, T. M.; Dawson, V. L.; El-Deiry, W. S.; Fulda, S.; Gottlieb, E.; Green, D. R.; Hengartner, M. O.; Kepp, O.; Knight, R. A.; Kumar, S.; Lipton, S. A.; Lu, X.; Madeo, F.; Malorni, W.; Mehlen, P.; Nunez, G.; Peter, M. E.; Piacentini, M.; Rubinsztein, D. C.; Shi, Y.; Simon, H.-U.; Vandenabeele, P.; White, E.; Yuan, J.; Zhivotovsky, B.; Melino, G.; Kroemer, G. *Cell Death Differ.* **2011**, 1.

57. Philchenkov, A. *Biochemistry (Moscow)* **2003**, *68*, 365.

58. Parrish, A. B.; Freel, C. D.; Kornbluth, S. *Cold Spring Harb. Perspect. Biol.* **2013**, *5*, a008672.

59. Castedo, M.; Perfettini, J. L.; Roumier, T.; Valent, A.; Raslova, H.; Yakushijin, K.; Horne, D.; Feunteun, J.; Lenoir, G.; Medema, R.; Vainchenker, W.; Kroemer, G. *Oncogene* **2004**, *23*, 4362.

60. Johnson, D. E.; Gastman, B. R.; Wieckowski, E.; Wang, G. Q.; Amoscato, A.; Delach, S. M.; Rabinowich, H. *Cancer Res.* **2000**, *60*, 1818.

61. Philchenkov, A.; Zavelevich, M.; Savinska, L.; Blokhin, D. *Exp. Oncol.* **2010**, *32*, 76.

62. Fang, L.; Shen, L.; Fang, Y.; Hu, Y.; He, Q.; Yang, B. *J. Cancer Res. Clin. Oncol.* **2008**, *134*, 1337.

63. Romagnoli, R.; Baraldi, P. G.; Salvador, M. K.; Camacho, M. E.; Preti, D.; Tabrizi, M. A.; Bassetto, M.; Brancale, A.; Hamel, E.; Bortolozzi, R.; Basso, G.; Viola, G. *Bioorg. Med. Chem.* **2012**, *20*, 7083.

64. Ho, L. H.; Read, S. H.; Dorstyn, L.; Lambrusco, L.; Kumar, S. *Oncogene* **2008**, *27*, 3393.

65. Zhu, H.; Zhang, J.; Xue, N.; Hu, Y.; Yang, B.; He, Q. *Invest. New Drugs* **2010**, *28*, 493.

66. Nabha, S. M.; Mohammad, R. M.; Dandashi, M. H.; Coupaye-Gerard, B.; Aboukameel, A.; Pettit, G. R.; Al-Katib, A. M. *Clin. Cancer Res.* **2002**, *8*, 2735.

67. Kepp, O.; Galluzzi, L.; Lipinski, M.; Yuan, J.; Kroemer, G. *Nat. Rev. Drug Discov. 2011, 10, 221-237* **2011**, *10*, 221.

68. Salway, A. H. *J. Chem. Soc. , Trans.* **1909**, *95*, 1178.

69. Piggott, M. J.; Wege, D. *Aust. J. Chem.* **2000**, *53*, 749.

70. Pietruszka, J.; Witt, A. *Synthesis* **2006**, *24*, 4266.

71. Jung, Y.-G.; Kang, H.-U.; Cho, H.-K.; Cho, C.-G. *Org. Lett.* **2011**, *13*, 5890.

72. Hadfield, J. A.; McGown, A. T. *Synthetic Commun.* **1998**, *28*, 1421.

73. Zharov, A. A.; Guzyaeva, I. A. *Russ. Chem. Bull.* **2010**, *59*, 1225.

74. Ko, S. C.; Johnson, V. L.; Chow, S. C. *Biochem. Biophys. Res. Commun.* **2000**, *270*, 1009.

75. Greenberg, C. S.; Craddock, P. R. *Clin. Chem.* **1982**, *28*, 1725.

Table 1

Effects of 1,2,3-triazole analogues of combretastatins on sea urchin embryos and human cancer cells

1,5-Diaryl-1,2,3-triazoles 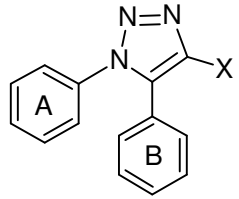

				Sea urchin embryo effects, EC (μM)[a]			NCI60 screen	
Compd	X	Ring A	Ring B	Cleavage alteration	Cleavage arrest	Embryo spinning	Mean GI_{50}, μM[b]	Mean GI, %[c]
CA4	-	3,4,5-triMeO-C_6H_2	3'-OH-4'-MeO-C_6H_3	0.002	0.01	0.05	0.0032[d]	
CA2	-	3,4-methylenedioxy-5-MeO-C_6H_2	3'-OH-4'-MeO-C_6H_3	0.002	0.01	0.05	2.66[e]	
5ad'	CN	3,4,5-triMeO-C_6H_2	4'-MeO-C_6H_4	> 4	> 4	> 4	ND[f]	
6ad'	$CONH_2$	3,4,5-triMeO-C_6H_2	4'-MeO-C_6H_4	> 4	> 4	> 4		101.06
7ad'	$COOCH_3$	3,4,5-triMeO-C_6H_2	4'-MeO-C_6H_4	> 4	> 4	> 4	ND[f]	
8ad'	COOH	3,4,5-triMeO-C_6H_2	4'-MeO-C_6H_4	> 4	> 4	> 4		99.38
9ad'	NH_2	3,4,5-triMeO-C_6H_2	4'-MeO-C_6H_4	0.1	> 4	> 5	ND[f]	
10ad'	H	3,4,5-triMeO-C_6H_2	4'-MeO-C_6H_4	0.02	0.2	1	0.027[g] 0.041[h]	
10bd'	H	3,4-methylenedioxy-5-MeO-C_6H_2	4'-MeO-C_6H_4	0.01	0.1	0.5	0.178	
10cd'	H	2,5-diMeO-3,4-methylenedioxy-C$_6$H	4'-MeO-C_6H_4	1	> 4	> 4	ND[f]	
5aa'	CN	3,4,5-triMeO-C_6H_2	3',4',5'-triMeO-C_6H_2	> 4	> 4	> 4		98.77

6aa'	$CONH_2$	3,4,5-triMeO-C_6H_2	3',4',5'-triMeO-C_6H_2	> 4	> 4	> 4			102.34
5da'	CN	4-MeO-C_6H_4	3',4',5'-triMeO-C_6H_2	1	> 4	> 4		ND[f]	
7da'	$COOC_2H_5$	4-MeO-C_6H_4	3',4',5'-triMeO-C_6H_2	> 4	> 4	> 4			104.13
8da'	COOH	4-MeO-C_6H_4	3',4',5'-triMeO-C_6H_2	> 4	> 4	> 4			103.52
9da'	NH_2	4-MeO-C_6H_4	3',4',5'-triMeO-C_6H_2	4	> 4	> 4			90.07
10da'	H	4-MeO-C_6H_4	3',4',5'-triMeO-C_6H_2	1	4	> 4	4[g]		
5dd'	CN	4-MeO-C_6H_4	4'-MeO-C_6H_4	4	> 4	> 4			96.66
5de'	CN	4-MeO-C_6H_4	3'-MeO-C_6H_4	0.2	1	5		ND[f]	
5fa'	CN	3-Cl-C_6H_4	3',4',5'-triMeO-C_6H_2	0.5	2	> 5			92.59
5fe'	CN	3-Cl-C_6H_4	3'-MeO-C_6H_4	> 4	> 4	> 4			92.04
7fg'	$COOC_2H_5$	3-Cl-C_6H_4	C_6H_5	> 4	> 4	> 4		ND[f]	
8fg'	COOH	3-Cl-C_6H_4	C_6H_5	> 4	> 4	> 4		ND[f]	
9fg'	NH_2	3-Cl-C_6H_4	C_6H_5	> 4	> 4	> 4		ND[f]	
10fg'	H	3-Cl-C_6H_4	C_6H_5	> 4	> 4	> 4		ND[f]	

4,5-Diaryl-1,2,3-triazoles

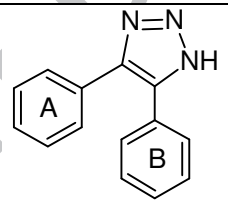

14ad'	–	3,4,5-triMeO-C_6H_2	4-MeO-C_6H_4	0.005	0.02	0.1	0.013[i]		
14bd'	–	3,4-methylenedioxy-5-MeO-C_6H_2	4-MeO-C_6H_4	0.0005	0.002	0.05	0.034		

14cd'	–	2,5-diMeO-3,4-methylenedioxy-C_6H	4-MeO-C_6H_4	0.5	> 4	> 5	0.813

[a] The sea urchin embryo assay was conducted as described previously.[44] Fertilized eggs and hatched blastulae were exposed to 2-fold decreasing concentrations of compounds. Duplicate measurements showed no differences in effective threshold concentration (EC) values.

[b] GI_{50}: concentration required for 50% cell growth inhibition.

[c] GI %: single dose inhibition of cell growth at 10 μM concentration.

[d] Data from ref [53].

[e] Mean value for seven human cancer cell lines.[54]

[f] ND: not determined.

[g] Data for K562 human leukemia cell line.[31]

[h] Mean value for four human cancer cell lines.[39]

[i] $GI_{50} < 0.01$ μM for 50 from 60 cancer cell lines.

Table 2.

Cell growth inhibition data for compounds **10bd'**, **14ad'**, **14bd'**, and **14cd'** (GI_{50}, μM) against a panel of 60 human cancer cell lines

Panel	Cell line	Cell growth inhibition (GI_{50}, μM)[a]				
		10bd'	**14ad'**	**14bd'**	**14cd'**	CA4[b]
Leukemia	CCRF-CEM	0.132	<0.01	0.026	0.684	0.003
	HL-60(TB)	0.051	<0.01	0.023	0.307	0.002
	K-562	0.041	<0.01	<0.01	0.493	0.002
	MOLT-4	0.122	0.012	0.063	0.529	0.003
	RPMI-8226	0.253	<0.01	0.033	0.816	0.003
	SR	0.041	<0.01	<0.01	0.304	0.003
Non-small cell lung cancer	A549/ATCC	0.088	<0.01	0.024	0.532	0.016
	EKVX	ND[c]	<0.01	ND[c]	2.79	0.086
	HOP-62	0.125	<0.01	<0.01	0.899	0.003
	HOP-92	ND[c]	<0.01	ND[c]	0.500	0.003
	NCI-H226	4.67	0.051	0.294	15.2	0.004
	NCI-H23	ND[c]	<0.01	0.033	1.00	0.003
	NCI-H322M	0.673	<0.01	0.057	2.89	0.007
	NCI-H460	0.055	<0.01	0.011	0.409	0.003
	NCI-H522	0.021	<0.01	<0.01	0.301	0.002
Colon cancer	COLO 205	0.053	0.033	0.255	0.884	0.1
	HCC-2998	0.258	<0.01	0.044	1.11	0.063
	HCT-116	0.064	<0.01	0.019	0.353	0.003
	HCT-15	0.045	<0.01	<0.01	0.454	0.004
	HT-29	0.040	<0.01	0.034	0.376	0.1

	KM12	0.060	<0.01	0.023	0.412	0.005
	SW-620	0.056	<0.01	0.014	0.385	0.003
CNS cancer	SF-268	0.611	0.021	0.101	4.02	0.006
	SF-295	0.073	<0.01	<0.01	0.356	0.004
	SF-539	0.095	<0.01	0.017	0.909	0.003
	SNB-19	>100	<0.01	ND[c]	1.80	0.004
	SNB-75	0.119	<0.01	0.016	0.437	0.008
	U251	ND[c]	<0.01	ND[c]	0.362	0.004
Melanoma	LOX IMVI	ND[c]	<0.01	ND[c]	0.547	0.003
	MALME-3M	ND[c]	ND[c]	ND[c]	0.766	0.02
	M14	0.061	<0.01	0.013	0.341	0.003
	MDA-MB-435	0.022	<0.01	<0.01	0.193	ND[c]
	SK-MEL-2	ND[c]	<0.01	ND[c]	0.326	0.004
	SK-MEL-28	0.725	ND[c]	0.035	1.78	0.008
	SK-MEL-5	0.235	<0.01	0.029	0.343	0.004
	UACC-257	74.9	<0.01	23.0	0.595	0.003
	UACC-62	0.072	<0.01	<0.01	0.420	0.006
Ovarian cancer	IGROV1	0.123	<0.01	0.023	0.720	0.015
	OVCAR-3	0.053	<0.01	0.010	0.363	0.002
	OVCAR-4	4.17	<0.01	0.518	4.68	0.014
	OVCAR-5	0.374	<0.01	0.049	3.63	0.1
	OVCAR-8	0.284	<0.01	0.040	1.32	0.003
	NCI/ADR-RES	0.038	<0.01	<0.01	0.296	ND[c]
	SK-OV-3	0.271	<0.01	0.023	0.854	0.059
Renal cancer	786-0	0.363	<0.01	0.032	1.40	0.1

	A498	0.049	<0.01	<0.01	0.353	0.006
	ACHN	0.607	0.015	0.040	6.79	0.006
	CAKI-1	0.098	<0.01	0.011	0.762	0.026
	RXF 393	0.157	<0.01	0.017	0.657	0.002
	SN12C	0.486	<0.01	0.061	4.67	0.006
	TK-10	ND[c]	<0.01	14.7	6.37	0.1
	UO-31	0.692	1.21	0.051	2.96	0.019
Prostate cancer	PC-3	0.150	0.043	0.035	1.93	ND[c]
	DU-145	0.232	<0.01	0.032	1.42	ND[c]
Breast cancer	MCF7	0.047	<0.01	<0.01	0.352	ND[c]
	MDA-MB-231/ATCC	0.135	<0.01	0.045	1.13	ND[c]
	HS 578T	0.154	<0.01	0.022	1.35	ND[c]
	BT-549	0.160	<0.01	0.121	0.345	ND[c]
	T-47D	ND[c]	2.66	ND[b]	0.716	ND[c]
	MDA-MB-468	0.062	<0.01	0.019	0.218	ND[c]

[a] GI_{50}: Concentration required for 50% cell growth inhibition.

[b] NCI data for CA4 NSC 613729.

[c] ND: not determined.

Figure legends

Figure 1. Structure of combretastatins and their *cis*-restricted 1,2,3-triazole analogues.

Figure 2. Cytotoxic effect of **10ad'** or CA4P in Jurkat and Jurkat/A4 cells. Cell viability was assessed by direct counting of trypan blue dye-excluding cells. EC_{50} values were determined by linear interpolation of cell survival data after 48 h of treatment. Error bars: mean±SD for three independent experiments.

Figure 3. Effects of **10ad'** on cell cycle distribution in Jurkat and Jurkat/A4 cells. Cells were treated for 24 h with **10ad'** or CA4P. DNA content was analyzed by staining with propidium iodide (PI). Error bars: mean±SD for three independent experiments.

Figure 4. Morphology of Jurkat and Jurkat/A4 cells treated with **10ad'** for 48 h. Untreated cells were used as control. Note the morphological features of abnormal mitosis: micronucleus (arrowhead) and small cell fragment with unequally segregated chromosomes enclosed by the membrane (asterisk). Condensed nuclei (arrows) indicate the early stages of apoptosis. May–Grunwald–Giemsa staining, × 100.

Figure 5. Representative examples of cell distribution according to their DNA content. Jurkat and Jurkat/A4 cells were treated with **10ad'** or CA4P at the indicated concentrations for 48 h. Untreated cells were used as control. M1 comprises hypodiploid DNA content.

Figure 6. Effect of pancaspase inhibitor z-VAD-fmk on hypodiploid (sub-G_1) cell formation in Jurkat and Jurkat/A4 cells treated with **10ad'**. The cells were preincubated with 50 μM z-VAD-fmk for 3 h followed by exposure to **10ad'** or CA4P for 24 h or 48 h. Untreated cells and cells treated with z-VAD-fmk only were used as controls. The percentage of hypodiploid cells was determined by flow cytometry. Error bars: mean±SD for three independent experiments. * $P<0.01$ as compared to cells without Z-VAD-fmk pretreatment.

Figure 7. Expression of initiator caspases (A) and anti-apoptotic proteins (B) in Jurkat and Jurkat/A4 cells treated with **10ad'** or CA4P. **10ad'** was used at 30 nM in Jurkat cells and at 300 nM in Jurkat/A4 cells. CA4P was used at 15 nM in Jurkat cells and 150 nM in Jurkat/A4 cells.

Cell lysates were analyzed by Western blotting. β-Actin served as the loading control.

Figure 8. Effects of CA4 and **10ad'** on active caspase-3 expression and PARP-1 processing. Jurkat and Jurkat/A4 cells were exposed to **10ad'** or CA4P as indicated; untreated cells were used as controls. Permeabilized cells were stained with FITC-conjugated MoAbs against active caspase-3 or cleaved PARP-1. The percentage of active caspase-3 or cleaved PARP-1 positive cells (M1) was determined by flow cytometry. Each histogram shows representative staining profiles for 20 000 cells per experiment.

Scheme 1. Reagents and conditions: Synthesis of 1,5-diaryl-1,2,3-triazoles **5**–**10**. (a) ref [51]; (b) Et_2NH;[52] (c) 96% H_2SO_4, rt, 10 h; (d) Et_2NH;[52] (e) (i) 15% KOH, EtOH, rt, overnight; (ii) 18% HCl; (f) (i) SO_2Cl_2, reflux, 2.5 h; (ii) NaN_3, acetone-water, 0 ºC, 80 min, then warm to rt; (iii) EtOH, reflux, 5 h; (iv) 1N NaOH, EtOH, reflux, 8 h; (g) heating at mp, 1–2 min.

Scheme 2. Reagents and conditions: Synthesis of 4,5-diaryl-1,2,3-triazoles **14**. (a) K_2CO_3, MeOH, rt, 48 h; (b) Et_2NH, $Pd(PPh_3)_4$, CuI, 50 ºC, 2 h, then rt, overnight; (c) DMF, 15000 bar, 100 ºC, 7 h; (d) H_2, Pd/C, MeOH, CF_3COOH, 20 bar, 55 ºC, 50 h.

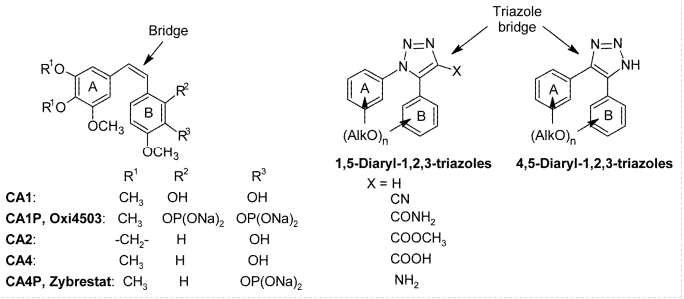

	R^1	R^2	R^3
CA1:	CH_3	OH	OH
CA1P, **Oxi4503**:	CH_3	$OP(ONa)_2$	$OP(ONa)_2$
CA2:	$-CH_2-$	H	OH
CA4:	CH_3	H	OH
CA4P, **Zybrestat**:	CH_3	H	$OP(ONa)_2$

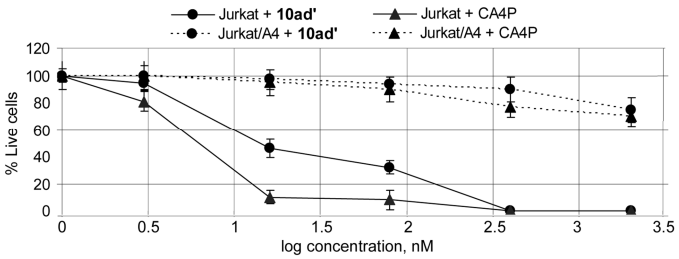

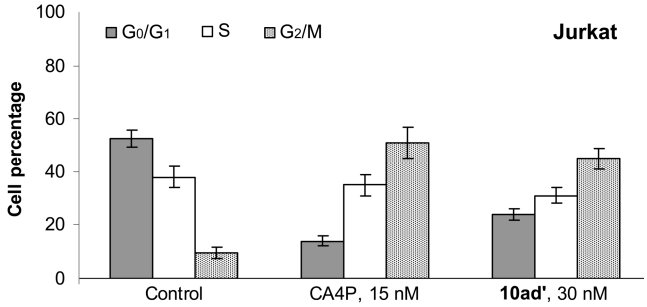

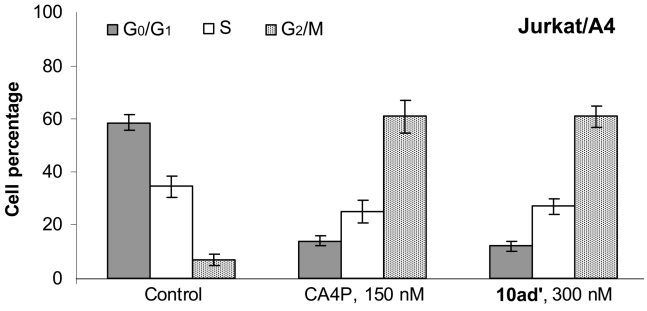

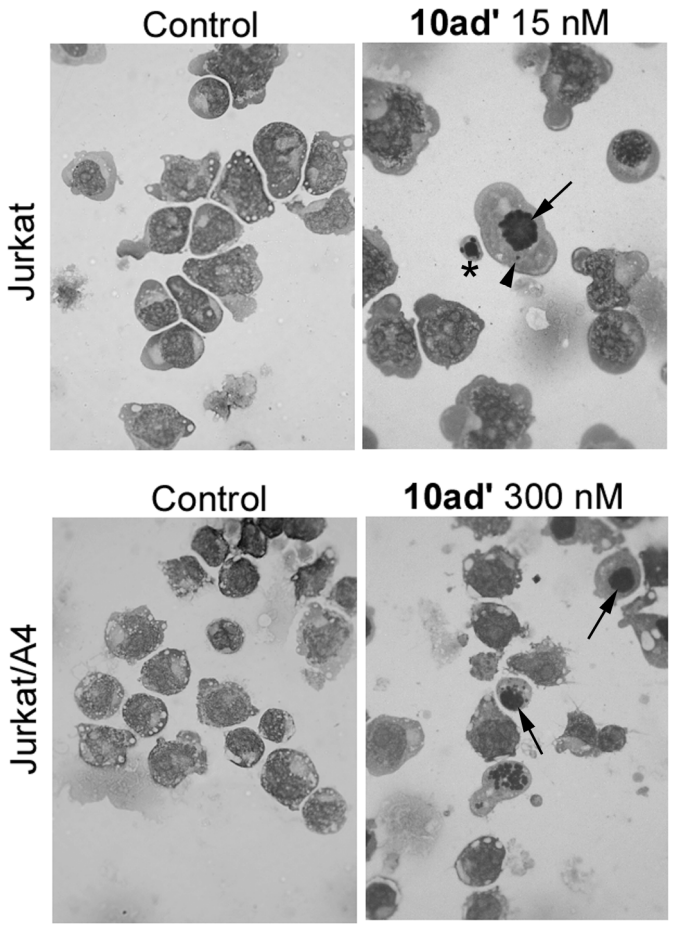

Jurkat

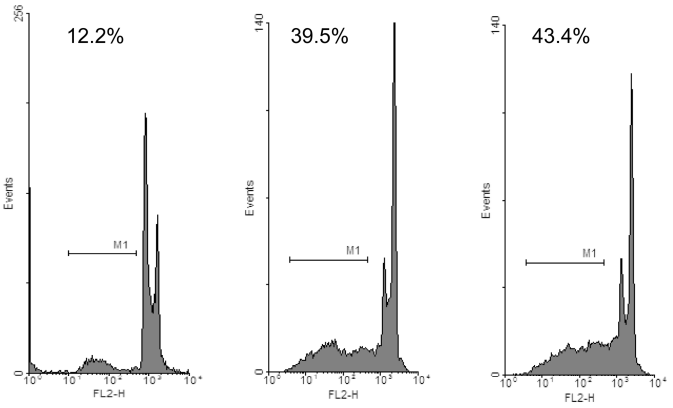

Control CA4P, 15 nM **10ad'**, 30 nM

Jurkat/A4

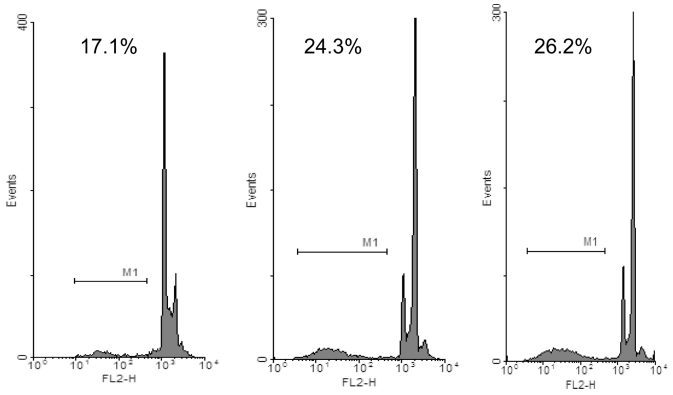

Control CA4P, 150 nM **10ad'**, 300 nM

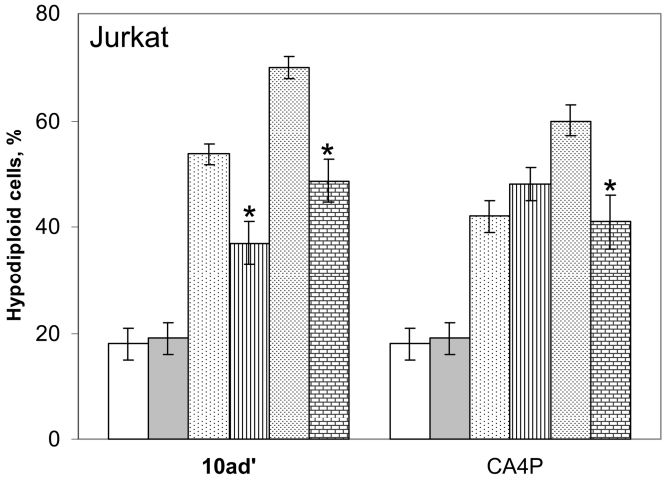

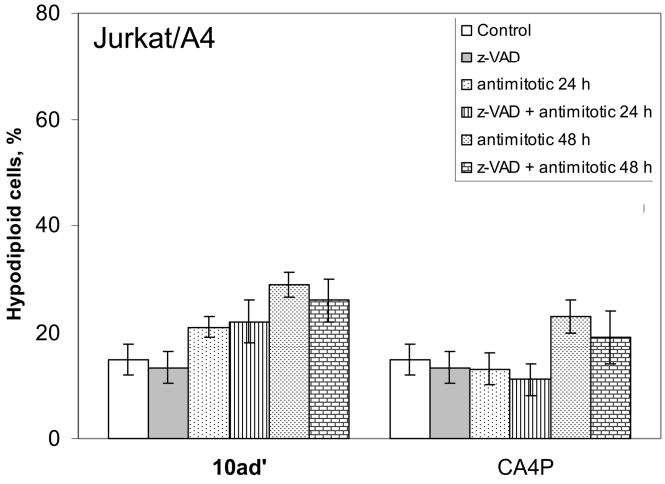

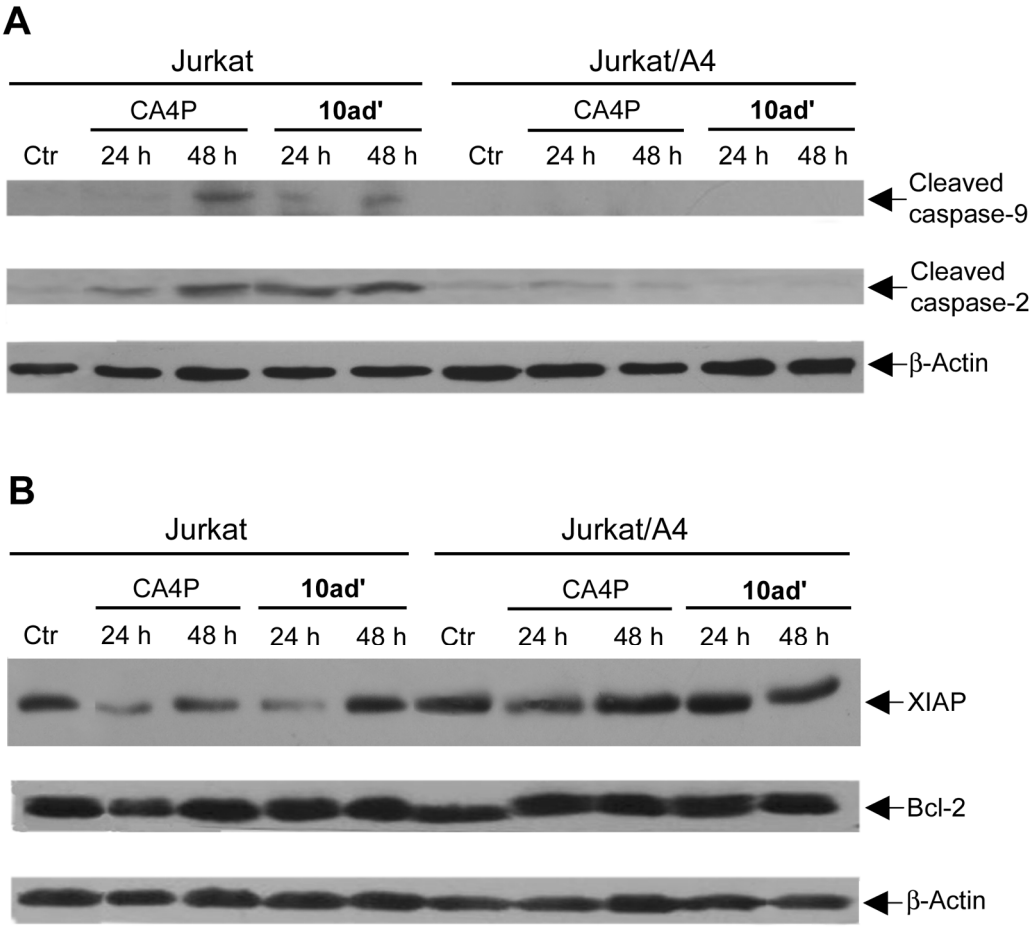

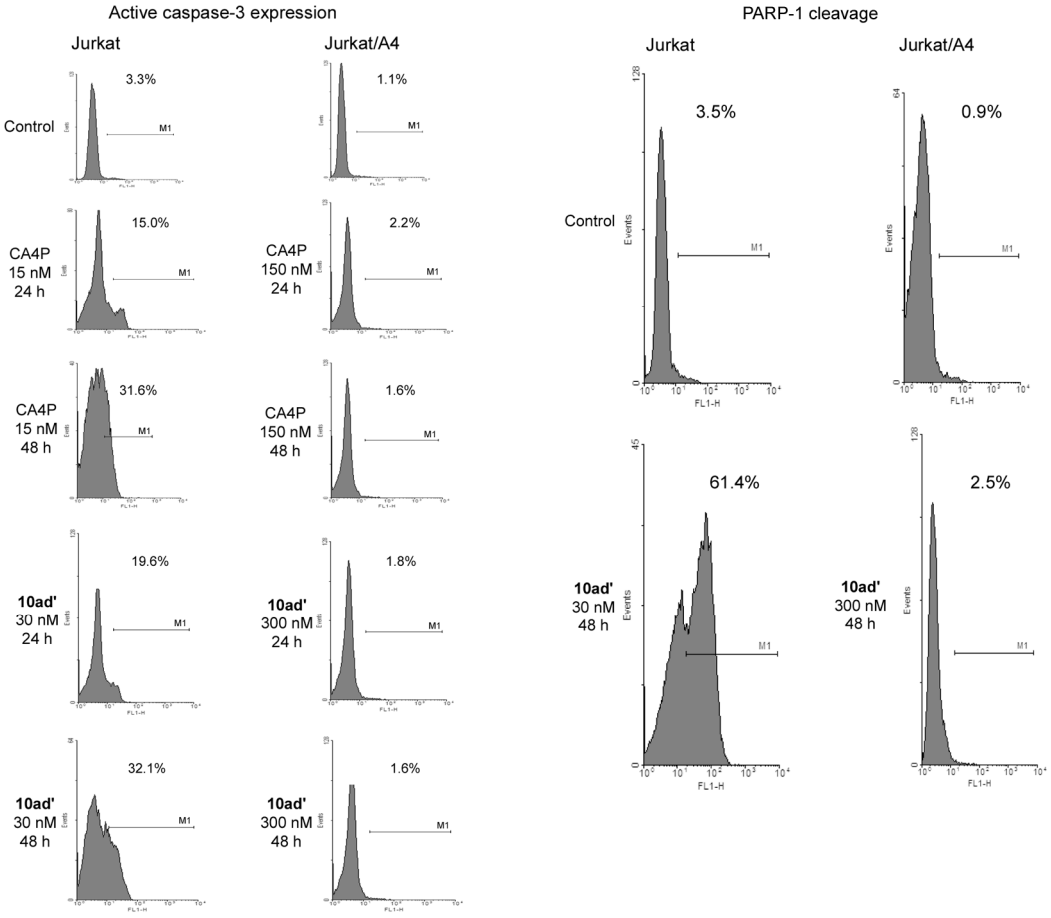

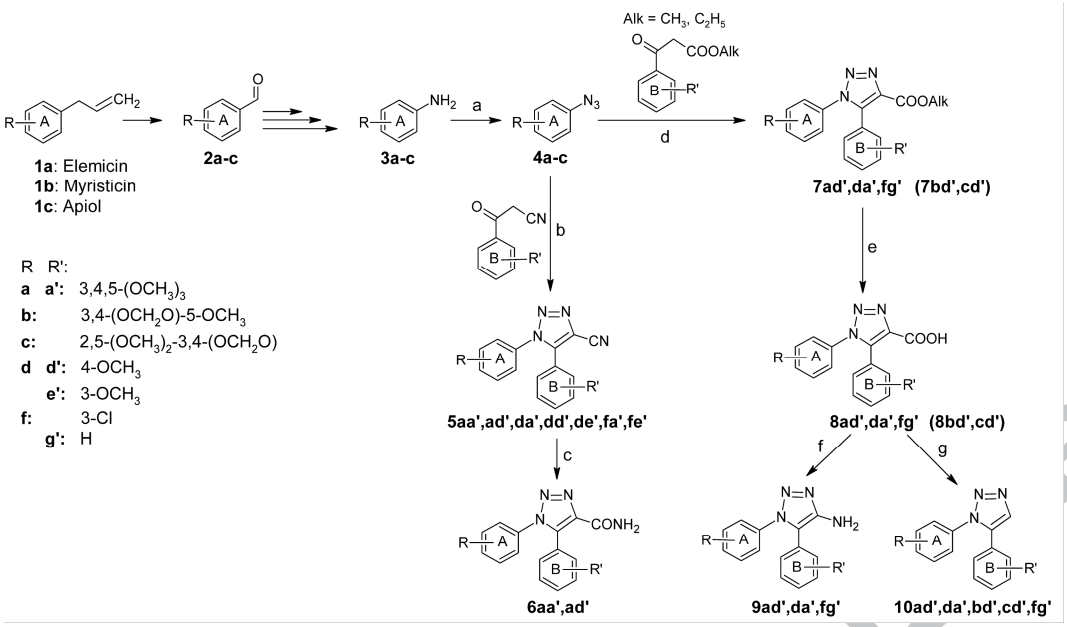

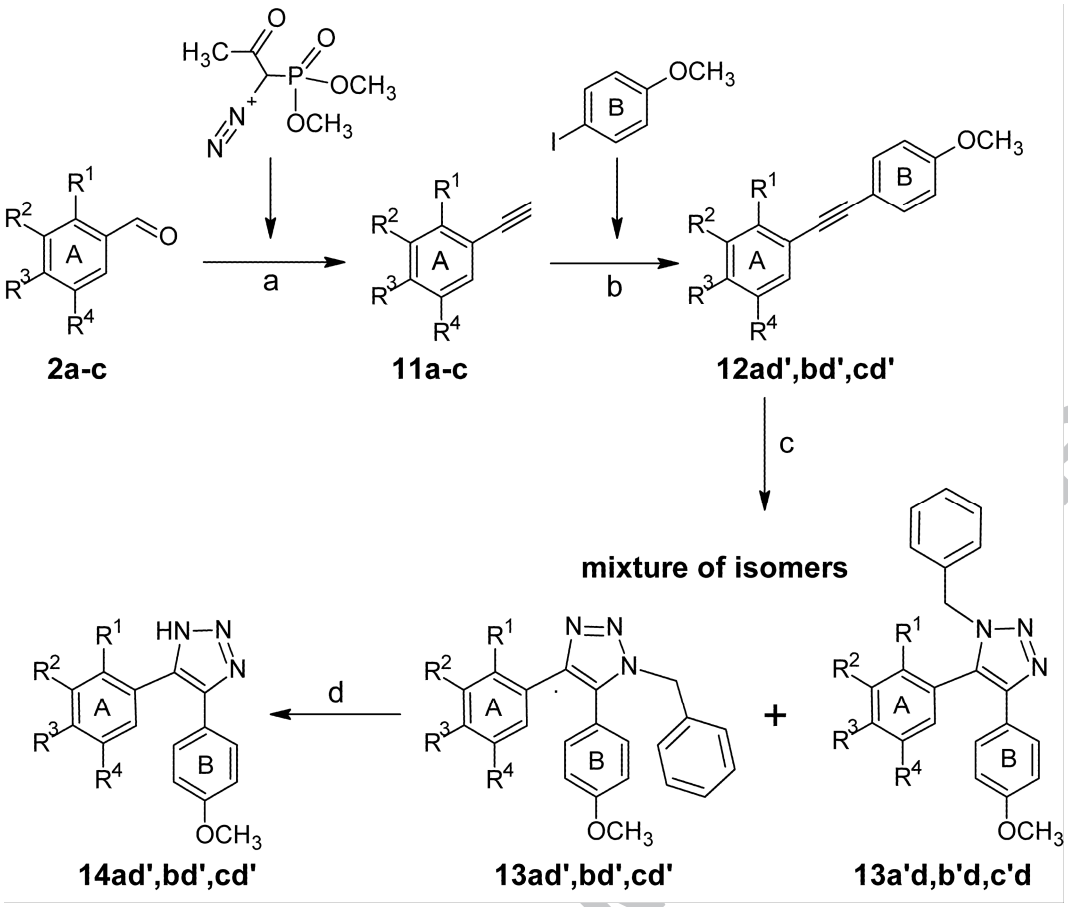

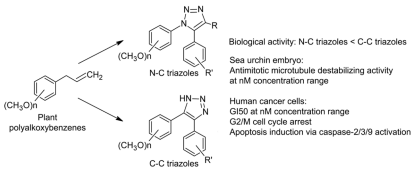

Biological activity: N-C triazoles < C-C triazoles

Sea urchin embryo:
Antimitotic microtubule destabilizing activity
at nM concentration range

Human cancer cells:
GI50 at nM concentration range
G2/M cell cycle arrest
Apoptosis induction via caspase-2/3/9 activation